Leukemia (2017), 1–9

www.nature.com/leu

ORIGINAL ARTICLE

Pan-mutant-IDH1 inhibitor BAY1436032 is highly effective against human IDH1 mutant acute myeloid leukemia *in vivo*

A Chaturvedi[1,10], L Herbst[2,10], S Pusch[3,4], L Klett[5], R Goparaju[1], D Stichel[3], S Kaulfuss[6], O Panknin[6], K Zimmermann[6], L Toschi[6], R Neuhaus[6], A Haegebarth[6], H Rehwinkel[6], H Hess-Stumpp[6], M Bauser[6], T Bochtler[2,7], EA Struys[8], A Sharma[1], A Bakkali[8], R Geffers[9], MM Araujo-Cruz[1], F Thol[1], R Gabdoulline[1], A Ganser[1], AD Ho[7], A von Deimling[3,4], K Rippe[5], M Heuser[1,11] and A Krämer[2,7,11]

Neomorphic mutations in isocitrate dehydrogenase 1 (*IDH1*) are frequently found in several human cancer types including acute myeloid leukemia (AML) and lead to the production of high levels of the oncometabolite (*R*)-2-hydroxyglutarate (R-2HG). Here we report the characterization of BAY1436032, a novel pan-mutant IDH1 inhibitor, both *in vitro* and *in vivo*. BAY1436032 specifically inhibits R-2HG production and colony growth, and induces myeloid differentiation of AML cells carrying IDH1R132H, IDH1R132C, IDH1R132G, IDH1R132L and IDH1R132S mutations. In addition, the compound impacts on DNA methylation and attenuates histone hypermethylation. Oral administration of BAY1436032 led to leukemic blast clearance, myeloid differentiation, depletion of leukemic stem cells and prolonged survival in two independent patient-derived xenograft IDH1 mutant AML mouse models. Together, BAY1436032 is highly effective against all major types of IDH1 mutant AML.

Leukemia advance online publication, 24 February 2017; doi:10.1038/leu.2017.46

INTRODUCTION

Isocitrate dehydrogenase (IDH) catalyzes the oxidative decarboxylation of isocitrate to α-ketoglutarate (αKG). Mutations in isocitrate dehydrogenase 1 (*IDH1*) and *IDH2* were found in several tumors including glioma,[1,2] acute myeloid leukemia (AML),[3] myeloproliferative neoplasm[4] and myelodysplastic syndrome patients,[5] chondrosarcoma,[6] lymphoma,[7] melanoma[8] and thyroid cancer.[9] Mutations in *IDH1* mostly occur at arginine 132, with substitutions including R132H, R132C, R132G, R132L and R132S, while mutations in *IDH2* occur at arginine 172 or arginine 140[(refs 10–12)] and affect the active sites, where IDH1/2 substrates isocitrate and $NADP^+$ bind.[13–16] Mutant IDH loses its normal activity with concomitant gain of a neomorphic function that catalyzes conversion of αKG to the oncometabolite (*R*)-2-hydroxyglutarate (R-2HG), which induces histone- and DNA hypermethylation through inhibition of demethylation, and leads to a block in cellular differentiation promoting tumorigenesis.[17–22] The prognostic significance of *IDH1* mutations in AML remains controversial, with a preponderance of studies suggesting that mutant IDH1 confers an adverse prognosis or has no prognostic value.[23] Serum R-2HG concentration may also serve as a prognostic indicator.[24–26]

AML treatment has not been significantly improved for the past four decades with the majority of patients eventually relapsing and dying of the disease. In cytogenetically normal AML, mutated *IDH1* is found in 10.9% of patients,[11] while mutated *IDH2* is found in 12.1%.[10] Recently, it has been shown that R-2HG, the oncometabolite produced by mutant IDH, promotes leukemogenesis even in the absence of mutant IDH and that pretreatment R-2HG serum levels impact on outcome in IDH1 mutant AML.[21,24] Previous studies have revealed that the mutant IDH enzyme remains important for the growth of IDH mutant cancers once they are fully established, and treatment with a mutant selective inhibitor induces cellular differentiation *ex vivo*.[21,27] We have also previously shown that pharmacological inhibition of the mutant IDH1 enzyme blocks colony formation of human AML cells but not of normal $CD34^+$ bone marrow cells *in vitro*.[28] Recently, a novel IDH1 inhibitor reduced 2-HG levels and induced differentiation *in vivo* after intraperitoneal administration in mice.[29] However, no beneficial effect of IDH1 inhibitors on survival of mice has been reported so far. The first clinical inhibitor of mutant IDH1, AG-120, induced complete remission in 18% and an overall response in 36% of patients.[30] An initial report of AG-120 treated patients showed that AML blasts differentiate to mature myeloid cells, but the allele burden of mutant IDH1 remained high in a considerable number of patients.[30] This suggests that inhibition of mutant IDH1 induces differentiation, but may not deplete leukemic stem cells *in vivo*. We developed a novel, highly active oral pan-IDH1 inhibitor, BAY1436032, and evaluated its preclinical activity in two independent patient-derived xenograft (PDX) AML mouse models. We show that BAY1436032 depletes AML cells in peripheral blood,

[1]Department of Hematology, Hemostasis, Oncology and Stem Cell Transplantation, Hannover Medical School, Hannover, Germany; [2]Clinical Cooperation Unit Molecular Hematology/Oncology, German Cancer Research Center (DKFZ) and Department of Internal Medicine V, University of Heidelberg, Heidelberg, Germany; [3]Department of Neuropathology, University of Heidelberg, Heidelberg, Germany; [4]Clinical Cooperation Unit Neuropathology, German Cancer Research Center (DKFZ) and German Cancer Consortium (DKTK), Heidelberg, Germany; [5]Research Group Genome Organization & Function, German Cancer Research Center (DKFZ) and Bioquant Center, Heidelberg, Germany; [6]Drug Discovery, Bayer Pharma AG, Berlin, Germany; [7]Department of Internal Medicine V, University of Heidelberg, Heidelberg, Germany; [8]Department of Clinical Chemistry, VU University Medical Center, Amsterdam, The Netherlands and [9]Genome Analysis, Helmholtz Centre for Infection Research, Braunschweig, Germany. Correspondence: Professor A Krämer, Clinical Cooperation Unit Molecular Hematology/Oncology, German Cancer Research Center (DKFZ) and Department of Internal Medicine V, University of Heidelberg, Im Neuenheimer Feld 280, Heidelberg 69120, Germany.
E-mail: a.kraemer@dkfz.de
[10]These authors contributed equally to this work.
[11]These senior authors contributed equally to this work.
Received 16 December 2016; revised 7 January 2017; accepted 13 January 2017; accepted article preview online 31 January 2017

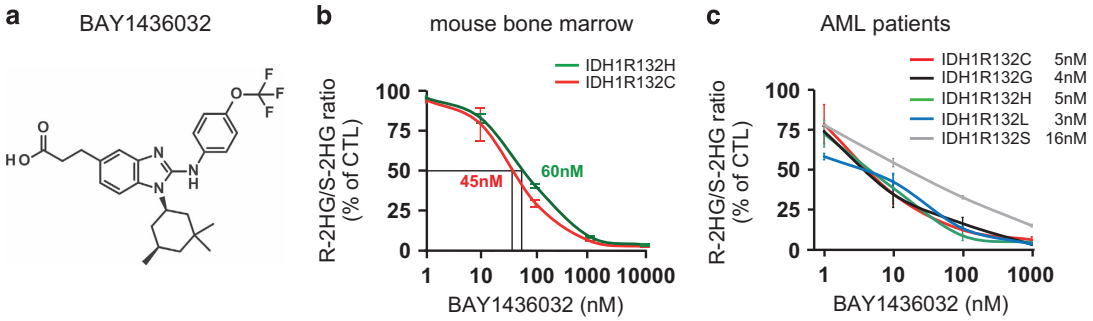

Figure 1. BAY1436032 selectively inhibits R-2HG production in IDH1 mutant mouse hematopoietic and primary human AML cells. (**a**) Chemical structure of BAY1436032. (**b**) Ratio of R-2HG to S-2-hydroxyglutarate (S-2HG) after 8 days of BAY1436032 treatment of HoxA9-immortalised mouse bone marrow cells retrovirally transduced with IDH1R132C or IDH1R132H. Half maximal inhibitory concentration (IC_{50}) values were calculated as percentage of dimethyl sulfoxide (DMSO; CTL) treatment and are indicated in the graph (mean ± s.e.m., $n = 3$). (**c**) Ratio of R-2HG to S-2HG in primary human AML cells harboring different IDH1 mutations 24 h after BAY1436032 treatment. IC_{50} values were calculated as percentage of DMSO (CTL) treatment and are given in the graph (mean ± s.e.m., $n = 3$).

prolongs survival, and inhibits leukemia stem cell (LSC) self-renewal *in vivo*.

MATERIALS AND METHODS

Cell culture and treatment

HoxA9-IDH1R132H, HoxA9-IDH1R132C, HoxA9-IDH2R140Q and HoxA9-IDH2172K cells were cultured in Dulbecco's modified Eagle's medium supplemented with 15% fetal bovine serum (FBS), 10 ng/ml of human interleukin 6 (hIL-6), 6 ng/ml of murine interleukin 3 (mIL-3), and 20 ng/ml of murine stem cell factor (mSCF; all from PeproTech, Hamburg, Germany) and were incubated at 37 °C with 5% CO_2 in humidified atmosphere. Patient-derived AML cells, freshly isolated or cryopreserved, were cultured in IMDM medium (Gibco, Karlsruhe, Germany) supplemented with 12.5% FBS (Gibco), 12.5% horse serum (Gibco), 5 μM hydrocortisone, 2.5 mM GlutaMax, 10 ng/ml human FLT3-ligand, 10 ng/ml human TPO, 50 ng/μl human SCF and 10 ng/μl human IL-3 (all from PeproTech) and were incubated at 37 °C with 5% CO_2 in humidified atmosphere. Treatment was carried out with BAY1436032 or dimethyl sulfoxide for indicated time points and concentrations.

Clonogenic progenitor assay

Colony-forming cell (CFC) units were assayed in methylcellulose (Methocult H4100; StemCell Technologies Inc., Cologne, Germany) supplemented with 10 ng/ml IL-3, 10 ng/ml GM-CSF, 50 ng/ml SCF, 50 ng/ml FLT3-ligand and 3 U/ml EPO (PeproTech). Vehicle or BAY1436032 was added to methylcellulose containing 10^5 human mononuclear cells, which were plated in duplicate. Colonies were evaluated microscopically 10 to 14 days after plating by standard criteria.

Antibodies for flow cytometry

Monoclonal antibodies used were CD45-FITC (2D1), CD45-PerCP-Cy5.5 (HI30), CD34-APC (8G12), CD34-FITC (HIT2), CD38-PE (HB-7), CD33-PE (WM53), CD14-APC (M5E2), CD14-FITC (M5E2), CD15-PE (W6D3), CD3-PE (UCHT1), CD19-APC (HIB19) from BD Biosciences (Heidelberg, Germany) and CD15-PE (80H5) from Beckman Coulter (Krefeld, Germany). Data were collected on either an Accuri C6 or a FACS Calibur (BD Biosciences).

RESULTS

On-target activity of BAY1436032, a novel IDH1 inhibitor, in IDH1-mutant hematopoietic cells

We developed a novel IDH1 inhibitor, BAY1436032, with high selectivity against all known IDH1R132 mutant proteins (R132H, R132C, R132G, R132S and R132L) compared to wild-type IDH1 and wild-type or mutant IDH2.[31] Details on chemical development, structural characteristics (Figure 1a) and activity profiles towards recombinant mutant and wild-type IDH1 and IDH2 proteins of BAY1436032 have been described by Pusch *et al.*[31] To assess the inhibitory effect of BAY1436032 on the enzymatic function of mutant IDH1 in a hematopoietic cell context, we employed immortalized mouse hematopoietic cells retrovirally engineered to express mutant IDH1 or IDH2, and primary human IDH1 or IDH2 mutant cells derived from AML patients. BAY1436032 inhibited intracellular R-2HG production in mouse hematopoietic cells expressing IDH1R132H or IDH1R132C with an IC_{50} of 60 and 45 nM, respectively (Figure 1b). In contrast, R-2HG levels were not reduced in IDH2R140Q and IDH2R172K expressing mouse hematopoietic cells by BAY1436032 at concentrations up to 10 μM (Supplementary Figure 1A). Patient-derived AML cells harboring IDH1R132C, IDH1R132G, IDH1R132H, IDH1R132L, or IDH1R132S mutations were very sensitive to BAY1436032 *ex vivo* with IC_{50} values between 3 and 16 nM whereas the compound had virtually no effect upon patient-derived AML cells with IDH2R140Q or IDH2R172K mutations at concentrations up to 1 μM (Figure 1c and Supplementary Figure 1B). Thus, BAY1436032 displays on-target activity towards mutant IDH1 in both mouse and primary human hematopoietic cells.

BAY1436032 inhibits proliferation and induces differentiation in primary human AML cells

Next, we assessed the effect of BAY1436032 on proliferation and differentiation of primary human AML cells with wild-type or mutant IDH1. Patient-derived AML cells harboring either wild-type IDH1 or IDH1R132H, IDH1R132C, IDH1R132L or IDH1R132S mutations were seeded in semi-solid medium supplemented with BAY1436032 at different concentrations or vehicle. Colony growth was inhibited by 50% at a concentration of 0.1 μM BAY1436032, while concentrations up to 100 μM did not suppress colony growth of patient-derived IDH1 wild-type AML cells (Figure 2a). IDH1 mutant AML cells cultured in suspension medium *ex vivo* showed marked upregulation of myeloid differentiation markers CD14 and CD15 (Figure 2b and Supplementary Figure 1C). On morphologic evaluation myelomonocytic differentiation of myeloid progenitors was strongly induced by BAY1436032 (Figure 2c). These data suggest that BAY1436032 inhibits proliferation and induces differentiation of primary IDH1 mutant AML cells *ex vivo*. As primary AML cells can only be propagated in culture for a limited time before spontaneous apoptosis occurs, we aimed to validate these findings *in vivo* in PDX AML mouse models.

Favorable pharmacokinetics allow once daily dosing of BAY1436032

A PDX mouse model was developed using primary AML cells from a patient with IDH1R132C mutant AML (PDX1). Targeted sequencing of the patient AML cells revealed a *FLT3*-TKD (p.D835del), an atypical *NPM1* (p.S254LfsTer4), and a *NRAS* (p.Q61R) mutation as

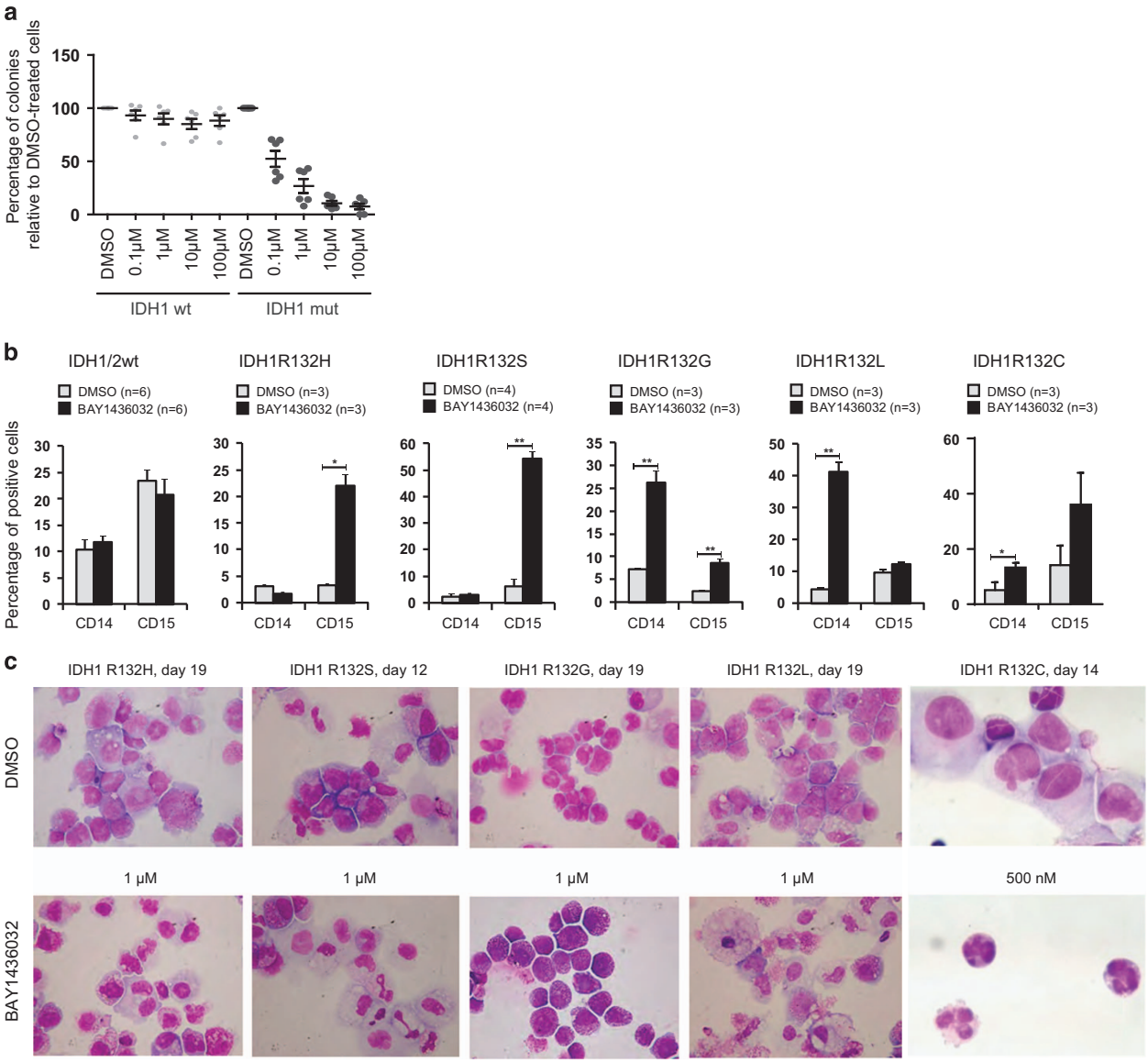

Figure 2. BAY1436032 inhibits proliferation and induces myeloid differentiation in patient-derived IDH1 mutant AML cells *ex vivo*. (**a**) Inhibition of colony formation by BAY1436032 in colony-forming cell assays using primary human AML cells with wild-type (wt) or mutant (mut) IDH1 (mean ± s.e.m., $n = 6$). From the six patients with IDH1 mutant AML, three harbored a IDH1R132H mutation and one each IDH1R132C, IDH1R132L and IDH1R132S mutations, respectively. (**b**) Quantification of IDH1 wild-type (wt) or IDH1 mutant primary AML cells expressing CD14 and CD15 after *ex vivo* treatment with dimethyl sulfoxide (DMSO) or BAY1436032 (mean ± s.e.m.). Numbers of patient samples examined are given in the graph. $^*P < 0.05$; $^{**}P < 0.01$. (**c**) Morphology of primary IDH1 mutant AML cells after *ex vivo* treatment with DMSO or BAY1436032 showing signs of monocytic/granulocytic maturation (×1000 or ×4000 magnification). Treatment durations and BAY1436032 concentrations are given in the graph.

additional aberrations. These cells were propagated in primary NSG recipient mice and upon stable engraftment retransplanted into secondary recipients, where the mutations initially found could be confirmed. The cells were then transplanted into tertiary recipients, which were used for treatment with BAY1436032. Plasma exposure of BAY1436032 was almost dose-linear between 45 and 150 mg/kg with unbound concentrations covering the *in vitro* R-2HG/S-2HG ratio IC_{50} for 24 h (Supplementary Figure 2A). At all tested doses of BAY1436032 R-2HG serum levels declined rapidly starting as early as three hours after application, reaching 5-, 6- and 7.5-fold reductions with 45, 90 and 150 mg/kg BAY1436032, respectively, after 24 h (Supplementary Figure 2B). Long-term exposure to once daily oral BAY1436032 revealed nearly complete suppression of R-2HG production with 150 mg/kg BAY1436032 (Supplementary Figures 2C and D). Therefore, the pharmaco kinetic profile allowed once daily oral dosing for subsequent PDX *in vivo* experiments (see also Pusch *et al.*[31]).

BAY1436032 clears AML blasts *in vivo* and prolongs survival in PDX models of IDH1 mutant AML

Next, NSG mice were transplanted with primary AML cells from a patient with IDH1R132C mutant AML as described above for the PDX1 mouse model. Per condition 10 mice were treated with vehicle, 45 or 150 mg/kg body weight BAY1436032 once daily by oral gavage for 150 days starting 17 days after transplantation (Figure 3a–c). Serum R-2HG levels constantly increased in vehicle-treated mice reaching 62 µM at day 90 (Figure 3a). At 90 days serum levels of R-2HG were significantly lower in both the 45 and

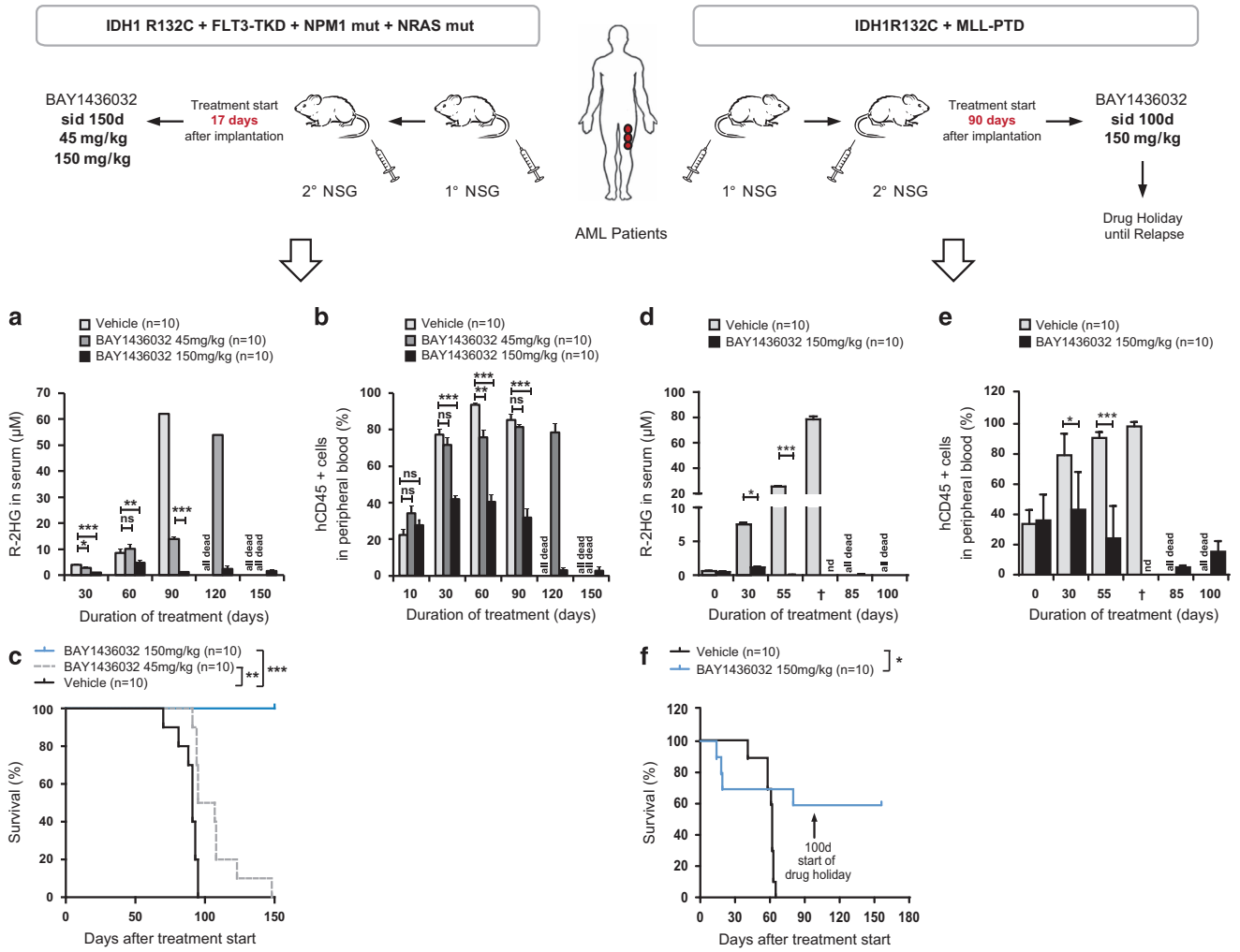

Figure 3. BAY1436032 exerts anti-leukemic activity in IDH1R132C AML PDX mouse models *in vivo*. The experimental setup of two independent PDX models is given at the top. (**a**) R-2HG serum levels of PDX1-IDH1R132C mice treated with 45 or 150 mg/kg of BAY1436032 or vehicle once daily. Serum was pooled from 3–4 mice for R-2HG measurements by mass spectrometry (mean ± s.e.m., $n = 10$). (**b**) Percentage of hCD45$^+$ leukemic cells in peripheral blood of PDX1-IDH1R132C mice at different time points after treatment start with 45 or 150 mg/kg of BAY1436032 or vehicle (mean ± s.e.m., $n = 10$). (**c**) Survival of PDX1-IDH1R132C mice treated with 45 or 150 mg/kg of BAY1436032 or vehicle ($n = 10$). (**d**) R-2HG serum levels of PDX2-IDH1R132C mice treated with 150 mg/kg of BAY1436032 or vehicle once daily. Serum was pooled from all mice and R-2HG was measured in technical triplicates by enzymatic assay (mean ± s.d., $n = 10$). (**e**) Percentage of hCD45$^+$ leukemic cells in peripheral blood of PDX2-IDH1R132C mice at different time points after treatment start with 150 mg/kg of BAY1436032 or vehicle (mean ± s.d., $n = 10$). (**f**) Survival of PDX2-IDH1R132C mice treated with 150 mg/kg of BAY1436032 or vehicle ($n = 10$). Treatment was stopped at day 100. *$P < 0.05$; **$P < 0.01$; ***$P < 0.001$; NS, not significant; ND, not determined; †, time of death.

150 mg/kg treatment groups (14 and 1 µM, respectively). Although serum R-2HG levels further increased in the 45 mg/kg group reaching 54 µM at day 120, R-2HG levels remained suppressed in the 150 mg/kg cohort until the end of the experiment at day 150. Accordingly, the percentage of human CD45$^+$ (hCD45$^+$) cells in the peripheral blood of the mice constantly increased in vehicle and 45 mg/kg BAY1436032 treated animals up to day 90, while it was significantly lower in the 150 mg/kg cohort and from day 30 onward declined to 2.8% at day 150 (Figure 3b). Similarly, white blood cell counts constantly increased in vehicle-treated mice and, at a lower rate, in animals receiving 45 mg/kg BAY1436032, while they remained constant in the 150 mg/kg cohort (Supplementary Figure 3A). Hemoglobin levels were slightly lower in the vehicle and 45 mg/kg groups as compared to the 150 mg/kg cohort at day 60 (Supplementary Figure 3B), while platelet counts were significantly reduced in vehicle and 45 mg/kg BAY1436032 treated mice compared to the 150 mg/kg cohort at day 60 (Supplementary Figure 3C). Strikingly, all mice receiving 150 mg/kg BAY1436032 survived with minimal hCD45$^+$ cell load in their peripheral blood until the end of observation at day 150 after treatment start ($P < 0.001$), while vehicle-treated animals died from leukemia with a median survival of 91 days. Mice receiving 45 mg/kg BAY1436032 showed a small but significant increase in survival to a median of 101 days ($P = 0.002$; Figure 3c).

In an independent second PDX model (PDX2), NSG mice were transplanted with primary IDH1R132C AML cells, which harbored a *MLL*-PTD mutation as additional recurrent aberration. Treatment with vehicle or 150 mg/kg BAY1436032 once daily by oral gavage for 100 days was initiated in this model at day 90 after transplantation, thereby more closely resembling the situation of AML patients at diagnosis or relapse (Figure 3d–f). Similar to the first model, serum R-2HG levels constantly increased in vehicle-treated mice reaching 78.5 µM at death (Figure 3d). Again, R-2HG serum levels remained suppressed in the 150 mg/kg cohort until the end of BAY1436032 treatment at day 100. Accordingly, the percentage of hCD45$^+$ cells in the peripheral blood of the mice constantly increased in vehicle-treated animals until death, while it was significantly lower in the BAY1436032 cohort and from day

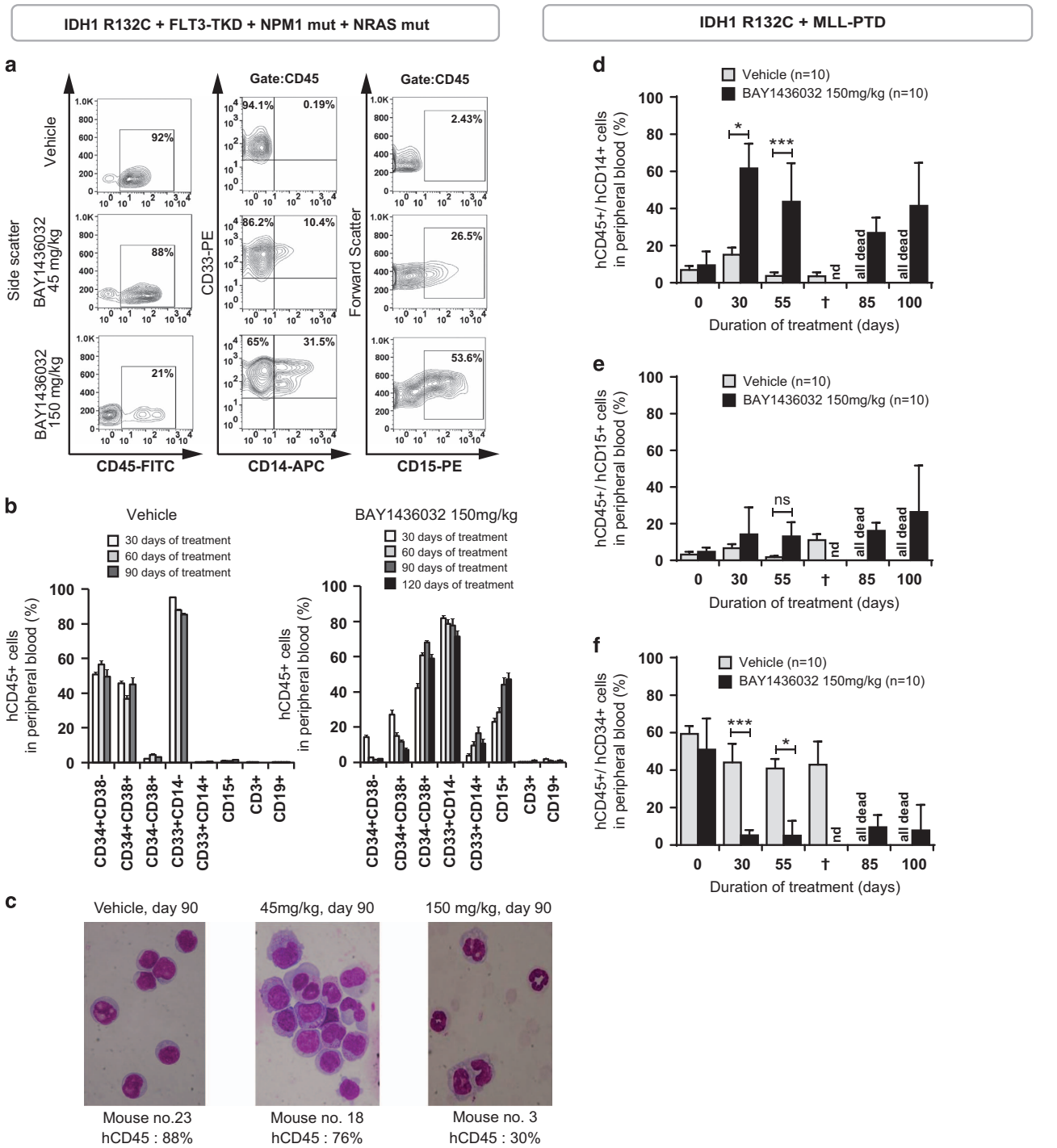

Figure 4. BAY1436032 induces myeloid differentiation of IDH1R132C mutant AML cells *in vivo*. (**a**) Representative FACS plots from peripheral blood cells of PDX1-IDH1R132C mice showing proportions of hCD45$^+$/CD14$^+$ and hCD45$^+$/CD15$^+$ cells at 90 days after treatment start with BAY1436032 or vehicle. (**b**) Immunophenotypes of hCD45$^+$ PDX1-IDH1R132C cells from mouse peripheral blood after treatment with vehicle (left) or 150 mg/kg BAY1436032 (right) at the indicated time points (mean ± s.e.m., $n = 10$). (**c**) Morphology of peripheral blood cells from PDX1-IDH1R132C mice treated with 45 or 150 mg/kg BAY1436032 or vehicle at the indicated time points (×1000 magnification). Percentages of hCD45$^+$/CD14$^+$ (**d**), hCD45$^+$/CD15$^+$ (**e**) and hCD45$^+$/CD34$^+$ (**f**) cells in the peripheral blood of PDX2-IDH1R132C mice treated with 150 mg/kg BAY1436032 or vehicle at the indicated time points after treatment start (mean ± s.d., $n = 10$). *$P < 0.05$; ***$P < 0.001$; NS, not significant; ND, not determined; †, time of death.

30 onward declined to 5.0% at day 85 and 15.3% at day 100 (Figure 3e). Total white blood cell counts increased in vehicle-treated mice until death, while they remained constantly low in the 150 mg/kg cohort (Supplementary Figure 3D). Both hemoglobin levels and platelet counts were reduced at death in the vehicle group while they remained constant in the 150 mg/kg cohort until the end of BAY1436032 treatment at day 100 (Supplementary Figures 3E and F). Although again all vehicle-treated mice died from leukemia with a median survival of 62 days, 6 of 10 animals receiving 150 mg/kg BAY1436032 survived until day 100, when

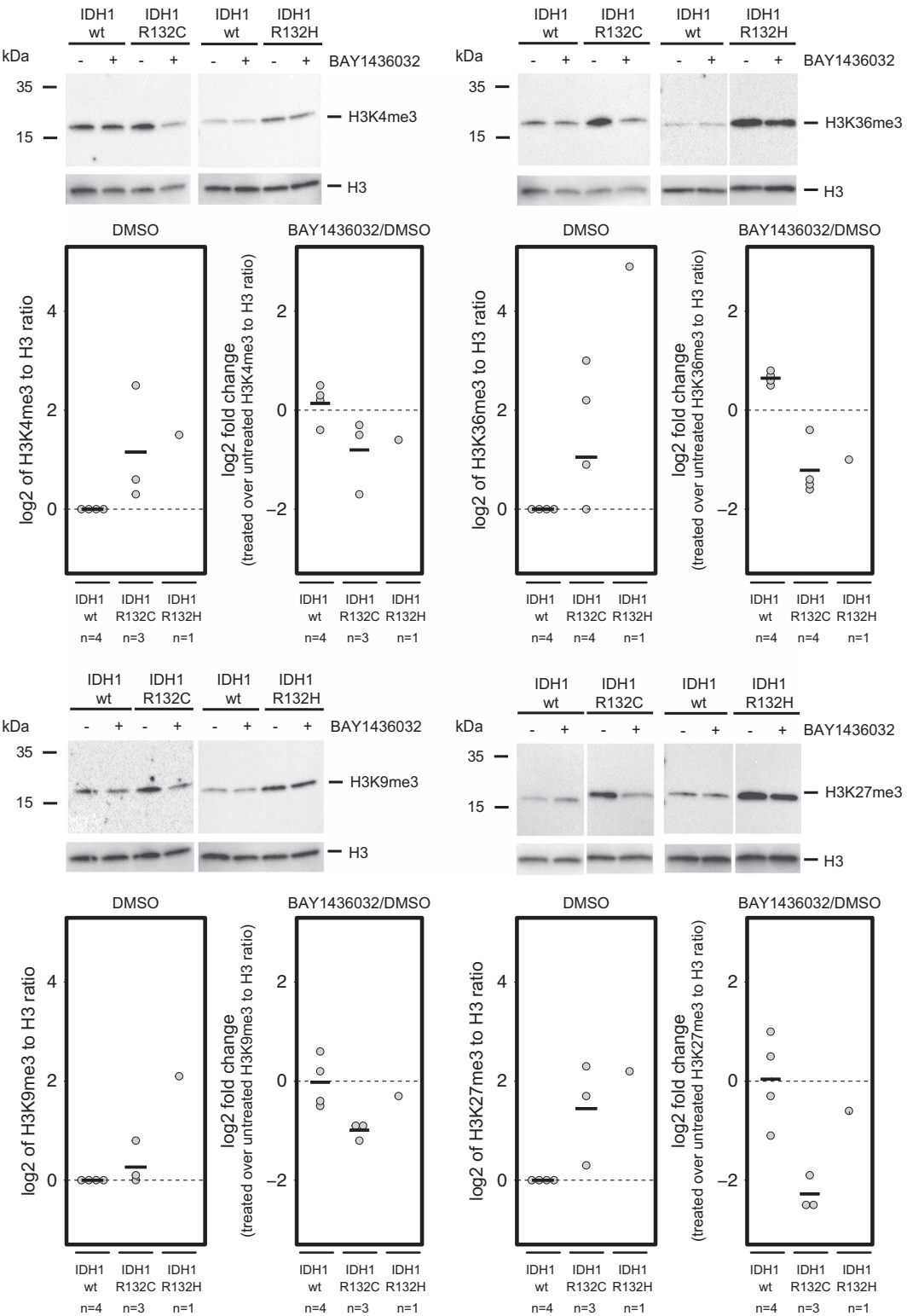

Figure 5. BAY1436032 impacts on histone methylation in patient-derived IDH1R132C and IDH1R132H mutant AML cells *ex vivo*. Western blots and quantification dot plots of histone H3 trimethylation levels at residues H3K4 (upper left), H3K36 (upper right), H3K9 (lower left) and H3K27 (lower right) in primary AML cells harboring wild-type (wt) IDH1 or IDH1R132C or IDH1R132H mutations. Cells were treated with 500 nM BAY1436032 or dimethyl sulfoxide (DMSO) as control for 14 days *ex vivo*. Log-transformed (base 2) ratios of the indicated histone modifications to total histone H3 levels in untreated IDH1 mutant cells compared to wild-type IDH1 cells (left panels) and log-transformed (base 2) fold changes of those ratios upon BAY1436032 treatment relative to DMSO control (right panels) were determined from the integrated intensity of the bands on the same western blot. The mean of logarithmized values is indicated for conditions with more than one measurement.

drug treatment was stopped (median survival not reached, $P = 0.014$; Figure 3f). Twenty-eight days after termination of BAY1436032 treatment the hCD45$^+$ cell load in the peripheral blood of the surviving six mice was still minimal and remained low in 4 of 6 animals at day 56 (Supplementary Figure 4). In an independent third PDX model, NSG mice were transplanted with primary wild-type IDH1/IDH2, NPM1 (p.W288CfsTer12) mutant AML cells (PDX3). Treatment with vehicle or 150 mg/kg BAY1436032 once daily by oral gavage was initiated at day 15 after transplantation. BAY1436032 and vehicle-treated mice had similar percentages of hCD45$^+$ cells, peripheral blood counts, spleen weight at death and survival, confirming the on-target activity of BAY1436032 (Supplementary Figure 5). We conclude that BAY1436032 exerts a striking and specific therapeutic effect at a dose of 150 mg/kg in PDX mouse models transplanted with primary human IDH1 mutant AML cells.

BAY1436032 induces myeloid differentiation in IDH1 mutant AML PDX models *in vivo*

To validate the induction of myelomonocytic differentiation by BAY1436032 *in vivo* the immunophenotype of hCD45$^+$ cells from the peripheral blood of NSG mice transplanted with IDH1R132C mutant AML cells carrying additional *FLT3*, *NPM1* and *NRAS* mutations (PDX1) was constantly monitored by flow cytometry. At day 90 after initiation of treatment, 94% of hCD45$^+$ cells in vehicle-treated mice co-expressed CD33 but myelomonocytic maturation markers CD14 ($0.5 \pm 0.5\%$, $n = 2$) and CD15 ($1.7 \pm 0.5\%$, $n = 2$) were completely absent (Figure 4a). In contrast, mice treated with 150 mg/kg BAY1436032 harbored only few hCD45$^+$ cells in their peripheral blood with a significant proportion of them co-expressing CD14 ($16.6 \pm 10.7\%$, $n = 2$) and CD15 ($44.2 \pm 11.6\%$, $n = 2$). Mice treated with 45 mg/kg BAY1436032 displayed intermediate levels of CD14/CD15 expression (Figure 4a). The immunophenotype of AML cells remained unchanged over time in vehicle-treated mice with high proportions of CD34$^+$CD38$^-$ and CD34$^+$CD38$^+$ progenitor cells (Figure 4b, left panel). Conversely, in mice treated with 150 mg/kg BAY1436032 the amount of CD34$^+$ CD38$^-$ and CD34$^+$CD38$^+$ cells rapidly decreased while CD34$^-$CD38$^+$, CD33$^+$CD14$^+$ and particularly CD15$^+$ cells increased (Figure 4b, right panel). Morphologic evaluation confirmed blastic morphology of peripheral blood cells in vehicle-treated cells, while some differentiation towards myelocytes was noted in the 45 mg/kg group. Bands and neutrophils were the predominant morphology in mice treated with 150 mg/kg BAY1436032 (Figure 4c).

Similarly, in the independent second PDX model of NSG mice transplanted with primary IDH1R132C AML cells and an additional *MLL*-PTD mutation (PDX2), the immunophenotype of AML cells in vehicle-treated mice remained virtually unchanged over time until death with regard to constantly high levels of CD34 co-expression and a lack of CD14/CD15 upregulation (Figure 4d-f). In contrast, the amount of CD34 co-expressing AML cells rapidly decreased while CD14$^+$ and CD15$^+$ cells increased in the 150 mg/kg BAY1436032 cohort. After termination of BAY1436032 treatment the few remaining hCD45$^+$ cells (Supplementary Figure 4A) in the peripheral blood of surviving mice progressively lost CD14 expression over time (Supplementary Figures 4B–D). Together, BAY1436032 induces myeloid differentiation at a dose of 150 mg/kg in two independent PDX mouse models transplanted with primary human IDH1 mutant AML cells.

BAY1436032 depletes leukemic stem cells by induction of myeloid differentiation and inhibition of cell cycle progression

To assess the effect on leukemic stem cell (LSC) self-renewal we treated NSG mice transplanted with primary human IDH1R132C mutant AML cells (PDX1) with 150 mg/kg BAY1436032 or vehicle for 4 weeks. Subsequently a limiting dilution transplantation experiment with 3 NSG recipient mice per cell dose (200 000, 20 000, 2000, 200 and 20 hCD45$^+$ cells per mouse) was performed. LSC frequency was determined using Poisson statistics. LSC frequency was 1 LSC in 84 hCD45$^+$ cells in vehicle-treated mice, while the frequency was approximately 100-fold lower in BAY1436032 treated animals (1 LSC in 8683 hCD45$^+$ cells, $P < 0.001$; Supplementary Figure 6A). Next, we performed gene expression profiling of hCD45$^+$ cells from NSG mice four weeks after treatment with vehicle or 150 mg/kg BAY1436032. Expression of stemness-associated genes including *SPARC*, *CD69* and *DNMT3B* was downregulated, while genes associated with myeloid differentiation and immune response were upregulated in BAY1436032 treated cells (GEO accession no. GSE83485; Supplementary Figures 6B and C and Supplementary Table 1). Gene set enrichment analysis revealed that one of the most highly enriched transcription factor gene sets upon treatment with BAY1436032 belonged to PU.1, while the top 20 gene sets for transcription factors that were negatively enriched in BAY1436032 treated cells were linked to the E2F family (Supplementary Figure 6D and Supplementary Table 2). Thus, BAY1436032 led to activation of the transcription factors PU.1, NFκB and AP1, while it inhibited E2F family transcription factors which promote progression from G_0/G_1 to S phase of the cell cycle (Supplementary Figure 6E). Accordingly, reduction of viable hCD45$^+$ cells in peripheral blood and bone marrow of NSG mice upon treatment with BAY1436032 (Supplementary Figure 6F) was paralleled by increased frequencies of hCD45$^+$ cells in G_0/G_1 and decreased frequencies in S phase of the cell cycle (Supplementary Figures 6G and 7). These data demonstrate that BAY1436032 not only induces differentiation but also inhibits cell cycle progression and self-renewal of LSCs *in vivo*.

BAY1436032 impacts on histone and DNA hypermethylation in primary human IDH1-mutated AML cells

The inhibition of histone demethylases by R-2HG results in a histone hypermethylation phenotype.[17–19] Accordingly, global histone H3 trimethylation levels at residues H3K4, H3K9, H3K27 and H3K36 were analyzed *ex vivo* by immunoblotting in primary human AML cells carrying either an IDH1R132C or an IDH1R132H mutation and compared to IDH1 wild-type AML cells. Levels were increased for all four histone methylation marks analyzed in cells with mutant IDH1 as compared to the corresponding global histone methylation levels in wild-type IDH1 AML cells (Figure 5). Upon treatment with 500 nM BAY1436032 for 14 days, histone trimethylation levels decreased in both IDH1R132C and IDH1R132H mutant AML cells but not in IDH1 wild-type cells (Figure 5). These results show that BAY1436032 is specific for IDH1 mutant cells and can revert their histone hypermethylation phenotype.

In addition to histone hypermethylation, human AML cells with *IDH1/IDH2* mutation show global DNA hypermethylation.[17,20] To test whether treatment with BAY1436032 alters DNA methylation, primary human AML cells carrying either an IDH1R132C or an IDH1R132H mutation were treated with 500 nM BAY1436032 for 14 days and subsequently subjected to analysis using the Illumina Infinium HumanMethylation450 platform. In this analysis BAY1436032 treated and vehicle-treated cells clustered together into clearly separable groups using Pearson correlation (Supplementary Figure 8A). In accordance with the gene expression profiling results, methylation of the PU.1 promoter decreased while E2F1 promoter methylation increased upon treatment with BAY1436032 (Supplementary Figures 8B–E). Together, these data demonstrate that BAY1436032 impacts on DNA methylation and suggests that the compound differentially alters methylation patterns to upregulate *PU.1* and downregulate *E2F* gene expression.

DISCUSSION

Here we show that BAY1436032 selectively inhibits mutant IDH1 leading to potent suppression of R-2HG production, inhibition of proliferation, and induction of myeloid differentiation in primary IDH1 mutant AML cells *in vitro*. In two independent PDX mouse models of primary IDH1 mutant AML BAY1436032 prolongs survival by causing blast clearance and myeloid differentiation as well as inhibition of stem cell self-renewal.

Several inhibitors of mutant IDH isoforms that block R-2HG production *in vitro* and *in vivo* have recently been described. The first potent and specific IDH1 inhibitors reported were AGI-5198[refs 32,33] and, subsequently, ML309.[34,35] These compounds specifically inhibited IDH1R132H and were shown to inhibit 2HG production and induce differentiation in glioma cells. Subsequently, Zheng and coworkers reported two potent inhibitors of IDH1R132H and IDH1R132C with greater than 60-fold selectivity relative to wild-type IDH1.[36] In a recent study the pan-IDH1 inhibitors GSK321 and GSK864 decreased R-2HG production in several different IDH1 mutant primary AML cells *ex vivo*.[29] *In vivo*, GSK864 reduced leukemic blast counts, but improved survival has not been reported for any of these compounds yet. AG-120, a selective, potent inhibitor of mutant IDH1, is currently in clinical development for the treatment of cancers with IDH1 mutations. Preliminary data show that it causes myeloid differentiation and induces remissions in up to 36% of IDH1 mutant AML patients.[30] However, the allele burden of mutant IDH1 remained high in several responding patients, suggesting that LSCs are not depleted.[30] Here we developed and evaluated the orally bioavailable pan-IDH1 inhibitor BAY1436032 for its anti-leukemic effect in PDX mouse models of primary human IDH1 mutant AML.

BAY1436032 specifically inhibited the mutant IDH1 enzyme and decreased intracellular R-2HG levels in both mouse hematopoietic cells transfected with mutant versions of IDH1 and primary AML cells with a wide range of different IDH1 mutations. Consequently, the compound enhanced myeloid differentiation both *in vitro* and *in vivo* along with decreased colony formation *in vitro* and reduced cell cycle progression and blast clearance *in vivo*. In tissue culture, BAY1436032 led to upregulation of the myelomonocytic markers CD14 and CD15, which was paralleled by morphologic differentiation. Similar observations in AML have been reported by others.[29] The differentiation block induced by mutant IDH1 might be due to histone hypermethylation with pronounced accumulation of trimethylated histones as reported previously.[17–20] We found here that treatment with BAY1436032 led to reduced levels of H3K4me3, H3K9me3, H3K27me3 and H3K36me3 marks in primary IDH1 mutant AML, analogous to what has been described for H3K9me2 by GSK321 in IDH1R132C expressing HT-1080 cells.[29]

In accordance with myeloid differentiation and reduced proliferation, gene expression profiling revealed that treatment of PDX mice with BAY1436032 led to reduced expression of stemness-associated genes and inhibition of E2F transcription factors. In contrast, the activity of myeloid transcription factors like PU.1 was upregulated in $hCD45^+$ AML cells. A similar cell cycle arrest in G_1 phase has been reported for IDH1 mutant AML cells treated with GSK321.[29] Although not significant, concordant demethylation of the PU.1 gene promoter and increased methylation of the E2F promoter was found by DNA methylation analysis. However, no significant difference in global DNA methylation was found, a result that is in line with the previous data from glioma xenotransplants treated with AGI-5198[ref. 33] or BAY1436032.[31]

Three other IDH1 inhibitors—AGI-5198, GSK321 and AG-120—have been shown to induce differentiation of IDH1 mutant glioma or AML cells.[29,30,33] Moreover, AG-120 was recently reported to even induce differentiation syndrome concurrently with clinical response in patients with IDH1 mutant AML.[37] Nevertheless, allele burden of mutant IDH1 remained high in these patients,[30] suggesting that AG-120 does not deplete LSCs. In contrast, BAY1436032 inhibits stem cell self-renewal as shown by low stem cell numbers in BAY1436032 treated mice upon secondary transplantation.

Myelomonocytic differentiation upon drug treatment occurred in both models and was similar to the *ex vivo* results. Reminiscent of clinical differentiation syndrome in AML patients treated with AG-120[37] we found an increased early mortality in our second PDX mouse model with primary IDH1R132C AML cells and an additional *MLL*-PTD mutation, in which mice suffered from a high leukemic burden when treatment was established at three months after transplantation. In contrast, in PDX1-IDH1R132C mice, which received BAY1436032 already at day 17 after transplantation, no early mortality occurred.

Once a day oral administration of 150 mg/kg BAY1436032 led to leukemic blast clearance and significantly prolonged survival in two independent PDX models of primary human IDH1 mutant AML. R-2HG production in PDX mice was rapidly inhibited after administration of BAY1436032. With 45 mg/kg BAY1436032 the reduction of R-2HG levels was first noted 7 h after treatment start. With 90 and 150 mg/kg, significant reduction of R-2HG levels occurred already 3 h after the first dose. While 45 mg/kg BAY1436032 only partially suppressed R-2HG production in long-term dosing experiments, it was insufficient to fully prevent expansion of leukemic cells and only moderately prolonged survival of PDX mice. In contrast, 150 mg/kg BAY1436032 led to almost complete suppression of R-2HG production, profound reduction of leukemic burden and significantly prolonged survival. Of note, even two months after termination of BAY1436032 treatment leukemic burden in the peripheral blood of two thirds of the remaining mice was still minimal, further arguing in favor of a significant depletion of the LSC pool.

In summary, the novel pan-mutant IDH1 inhibitor BAY1436032 is active against all IDH1R132 mutations and, when orally applied at a dose of 150 mg/kg, shows strong anti-leukemic activity in two independent AML PDX mouse models. On the basis of the present work on BAY1436032 a clinical phase one trial enrolling patients with IDH1R132 mutant AML is currently being initiated.

CONFLICT OF INTEREST

MH received research support from Bayer. The remaining authors declare no conflict of interest.

ACKNOWLEDGEMENTS

We acknowledge assistance of the Cell Sorting Core Facility of Hannover Medical School supported in part by the Braukmann–Wittenberg–Herz–Stiftung and the Deutsche Forschungsgemeinschaft. We thank all participating patients and contributing doctors, the staff of the Central Animal Facilities of Hannover Medical School and German Cancer Research Center (DKFZ), and R. Schottmann, K. Görlich, S. Glowotz, M. Wichmann, J. Eisel and S. Schumacher for support. This work was supported by grants from the DKFZ-Bayer Alliance, an ERC grant under the European Union's Horizon 2020 research and innovation programme (No. 638035), by grants 110284, 110287, 110292 and 111267 from Deutsche Krebshilfe; grant DJCLS R13/14 from the Deutsche José Carreras Leukämie-Stiftung e.V; the German Federal Ministry of Education and Research grant 01EO0802 (IFB-Tx); DFG grants KR1981/4-1, HE5240/5-1 and HE5240/6-1; grants from Wilhelm Sander-Stiftung, Dieter-Schlag Stiftung, a HiLF grant from Hannover Medical School awarded to AC, and a Stiftung für Krebs- und Scharlachforschung Mannheim grant to LH.

AUTHOR CONTRIBUTIONS

AK, MH, AC and LH conceived and designed the study; AC, LH, SP, LK, RG, DS, SK, TB, EAS, AS, AB, RG, MMA-C, FT, RG, AG, ADH, AD, KR, MH and AK collected, analyzed, and assembled the data; OP, KZ, LT, RN, AH, HR, HH-S and MB provided critical reagents; AK and MH wrote the manuscript; and all authors reviewed the data, and edited and approved the final version of the manuscript.

REFERENCES

1 Parsons DW, Jones S, Zhang X, Lin JC, Leary RJ, Angenendt P *et al.* An integrated genomic analysis of human glioblastoma multiforme. *Science* 2008; **321**: 1807–1812.
2 Yan H, Parsons DW, Jin G, McLendon R, Rasheed BA, Yuan W *et al.* IDH1 and IDH2 mutations in gliomas. *N Engl J Med* 2009; **360**: 765–773.
3 Mardis ER, Ding L, Dooling DJ, Larson DE, McLellan MD, Chen K *et al.* Recurring mutations found by sequencing an acute myeloid leukemia genome. *N Engl J Med* 2009; **361**: 1058–1066.
4 Green A, Beer P. Somatic mutations of IDH1 and IDH2 in the leukemic transformation of myeloproliferative neoplasms. *N Engl J Med* 2010; **362**: 369–370.
5 Thol F, Weissinger EM, Krauter J, Wagner K, Damm F, Wichmann M *et al.* IDH1 mutations in patients with myelodysplastic syndromes are associated with an unfavorable prognosis. *Haematologica* 2010; **95**: 1668–1674.
6 Amary MF, Bacsi K, Maggiani F, Damato S, Halai D, Berisha F *et al.* IDH1 and IDH2 mutations are frequent events in central chondrosarcoma and central and periosteal chondromas but not in other mesenchymal tumours. *J Pathol* 2011; **224**: 334–343.
7 Cairns RA, Iqbal J, Lemonnier F, Kucuk C, de Leval L, Jais JP *et al.* IDH2 mutations are frequent in angioimmunoblastic T-cell lymphoma. *Blood* 2012; **119**: 1901–1903.
8 Shibata T, Kokubu A, Miyamoto M, Sasajima Y, Yamazaki N. Mutant IDH1 confers an in vivo growth in a melanoma cell line with BRAF mutation. *Am J Pathol* 2011; **178**: 1395–1402.
9 Murugan AK, Bojdani E, Xing M. Identification and functional characterization of isocitrate dehydrogenase 1 (IDH1) mutations in thyroid cancer. *Biochem Biophys Res Commun* 2010; **393**: 555–559.
10 Thol F, Damm F, Wagner K, Göhring G, Schlegelberger B, Hölzer D *et al.* Prognostic impact of IDH2 mutations in cytogenetically normal acute myeloid leukemia. *Blood* 2010; **116**: 614–616.
11 Wagner K, Damm F, Göhring G, Gorlich K, Heuser M, Schäfer I *et al.* Impact of IDH1 R132 mutations and an IDH1 single nucleotide polymorphism in cytogenetically normal acute myeloid leukemia: SNP rs11554137 is an adverse prognostic factor. *J Clin Oncol* 2010; **28**: 2356–2364.
12 Paschka P, Schlenk RF, Gaidzik VI, Habdank M, Kronke J, Bullinger L *et al.* IDH1 and IDH2 mutations are frequent genetic alterations in acute myeloid leukemia and confer adverse prognosis in cytogenetically normal acute myeloid leukemia with NPM1 mutation without FLT3 internal tandem duplication. *J Clin Oncol* 2010; **28**: 3636–3643.
13 Ward PS, Patel J, Wise DR, Abdel-Wahab O, Bennett BD, Coller HA *et al.* The common feature of leukemia-associated IDH1 and IDH2 mutations is a neomorphic enzyme activity converting alpha-ketoglutarate to 2-hydroxyglutarate. *Cancer Cell* 2010; **17**: 225–234.
14 Dang L, White DW, Gross S, Bennett BD, Bittinger MA, Driggers EM *et al.* Cancer-associated IDH1 mutations produce 2-hydroxyglutarate. *Nature* 2010; **465**: 966.
15 Gross S, Cairns RA, Minden MD, Driggers EM, Bittinger MA, Jang HG *et al.* Cancer-associated metabolite 2-hydroxyglutarate accumulates in acute myelogenous leukemia with isocitrate dehydrogenase 1 and 2 mutations. *J Exp Med* 2010; **207**: 339–344.
16 Sellner L, Capper D, Meyer J, Langhans CD, Hartog CM, Pfeifer H *et al.* Increased levels of 2-hydroxyglutarate in AML patients with IDH1-R132H and IDH2-R140Q mutations. *Eur J Haematol* 2010; **85**: 457–459.
17 Sasaki M, Knobbe CB, Munger JC, Lind EF, Brenner D, Brüstle A *et al.* IDH1(R132H) mutation increases murine haematopoietic progenitors and alters epigenetics. *Nature* 2012; **488**: 656–659.
18 Lu C, Ward PS, Kapoor GS, Rohle D, Turcan S, Abdel-Wahab O *et al.* IDH mutation impairs histone demethylation and results in a block to cell differentiation. *Nature* 2012; **483**: 474–478.
19 Turcan S, Rohle D, Goenka A, Walsh LA, Fang F, Yilmaz E *et al.* IDH1 mutation is sufficient to establish the glioma hypermethylator phenotype. *Nature* 2012; **483**: 479–483.
20 Figueroa ME, Abdel-Wahab O, Lu C, Ward PS, Patel J, Shih A *et al.* Leukemic IDH1 and IDH2 mutations result in a hypermethylation phenotype, disrupt TET2 function, and impair hematopoietic differentiation. *Cancer Cell* 2010; **18**: 553–567.
21 Losman JA, Looper RE, Koivunen P, Lee S, Schneider RK, McMahon C *et al.* (R)-2-hydroxyglutarate is sufficient to promote leukemogenesis and its effects are reversible. *Science* 2013; **339**: 1621–1625.
22 Chaturvedi A, Araujo Cruz MM, Jyotsana N, Sharma A, Goparaju R, Schwarzer A *et al.* Enantiomer-specific and paracrine leukemogenicity of mutant IDH metabolite 2-hydroxyglutarate. *Leukemia* 2016; **30**: 1708–1715.
23 Medeiros BC, Fathi AT, DiNardo CD, Pollyea DA, Chan SM, Swords R. Isocitrate dehydrogenase mutations in myeloid malignancies. *Leukemia* 2016; **31**: 272–281.
24 Balss J, Thiede C, Bochtler T, Okun JG, Saadati M, Benner A *et al.* Pretreatment D-2-hydroxyglutarate serum levels negatively impact on outcome in IDH1-mutated acute myeloid leukemia. *Leukemia* 2016; **30**: 782–788.
25 Wang JH, Chen WL, Li JM, Wu SF, Chen TL, Zhu YM *et al.* Prognostic significance of 2-hydroxyglutarate levels in acute myeloid leukemia in China. *Proc Natl Acad Sci USA* 2013; **110**: 17017–17022.
26 DiNardo CD, Propert KJ, Loren AW, Paietta E, Sun Z, Levine RL *et al.* Serum 2-hydroxyglutarate levels predict isocitrate dehydrogenase mutations and clinical outcome in acute myeloid leukemia. *Blood* 2013; **121**: 4917–4924.
27 Wang F, Travins J, DeLaBarre B, Penard-Lacronique V, Schalm S, Hansen E *et al.* Targeted inhibition of mutant IDH2 in leukemia cells induces cellular differentiation. *Science* 2013; **340**: 622–626.
28 Chaturvedi A, Araujo Cruz MM, Jyotsana N, Sharma A, Yun H, Görlich K *et al.* Mutant IDH1 promotes leukemogenesis in vivo and can be specifically targeted in human AML. *Blood* 2013; **122**: 2877–2887.
29 Okoye-Okafor UC, Bartholdy B, Cartier J, Gao EN, Pietrak B, Rendina AR *et al.* New IDH1 mutant inhibitors for treatment of acute myeloid leukemia. *Nat Chem Biol* 2015; **11**: 878–886.
30 DiNardo C, de Botton S, Pollyea DA, Stein EM, Fathi AT, Roboz GJ *et al.* Molecular profiling and relationship with clinical response in patients with IDH1 mutation-positive hematologic malignancies receiving AG-120, a first-in-class potent inhibitor of mutant IDH1, in addition to data from the completed dose escalation portion of the phase 1 study. *Blood* 2015; **126**: 1306.
31 Pusch S, Krausert S, Fischer V, Balss J, Ott M, Schrimpf D *et al.* Pan-mutant IDH1 inhibitor BAY 1436032 for effective treatment of IDH1 mutant astrocytoma *in vivo*. *Acta Neuropathol* 2017; e-pub ahead of print 25 January 2017; doi:10.1007/s00401-017-1677-y.
32 Popovici-Muller J, Saunders JO, Salituro FG, Travins JM, Yan S, Zhao F *et al.* Discovery of the first potent inhibitors of mutant IDH1 that lower tumor 2-HG in vivo. *ACS Med Chem Lett* 2012; **3**: 850–855.
33 Rohle D, Popovici-Muller J, Palaskas N, Turcan S, Grommes C, Campos C *et al.* An inhibitor of mutant IDH1 delays growth and promotes differentiation of glioma cells. *Science* 2013; **340**: 626–630.
34 Davis M, Pragani R, Popovici-Muller J, Gross S, Thorne N, Salituro F *et al. ML309: A Potent Inhibitor of R132H Mutant IDH1 Capable of Reducing 2-Hydroxyglutarate Production in U87 MG Glioblastoma Cells*. Probe Reports from the NIH Molecular Libraries Program: Bethesda, USA, 2010.
35 Davis MI, Gross S, Shen M, Straley KS, Pragani R, Lea WA *et al.* Biochemical, cellular, and biophysical characterization of a potent inhibitor of mutant isocitrate dehydrogenase IDH1. *J Biol Chem* 2014; **289**: 13717–13725.
36 Zheng B, Yao Y, Liu Z, Deng L, Anglin JL, Jiang H *et al.* Crystallographic investigation and selective inhibition of mutant isocitrate dehydrogenase. *ACS Med Chem Lett* 2013; **4**: 542–546.
37 Birendra KC, DiNardo CD. Evidence for clinical differentiation and differentiation syndrome in patients with acute myeloid leukemia and IDH1 mutations treated with the targeted mutant IDH1 inhibitor, AG-120. *Clin Lymphoma Myeloma Leuk* 2016; **16**: 460–465.

Supplementary Information accompanies this paper on the Leukemia website (http://www.nature.com/leu)

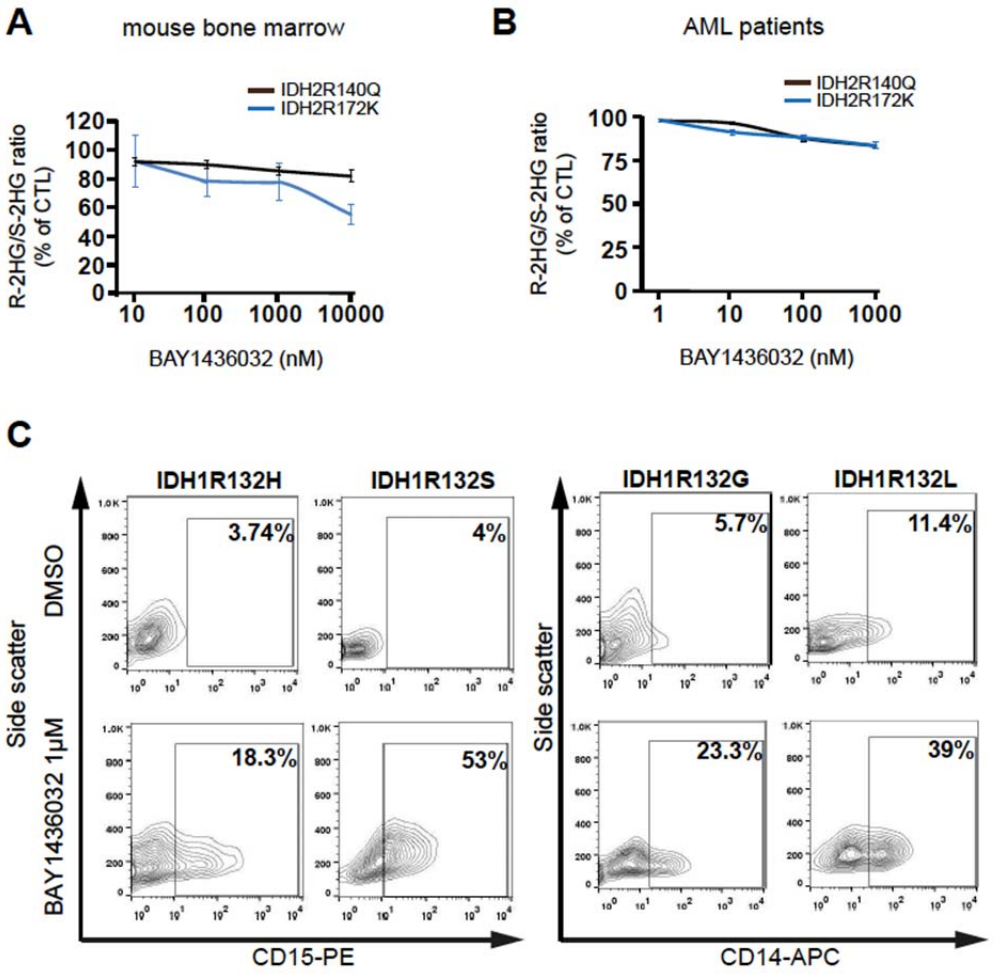

Supplementary Figure 1. BAY1436032 selectively inhibits R-2HG production and induces myeloid differentiation in IDH1 mutant mouse hematopoietic and primary human AML cells. (**A**) Ratio of R-2HG to S-2HG after 8 days of BAY1436032 treatment of HoxA9-immortalized mouse bone marrow cells retrovirally transduced with IDH2R140Q or IDH2R172K. Intracellular R-2HG/S-2HG ratios were calculated as percentage of DMSO (CTL) treatment (mean ± SEM, *n* = 3). (**B**) Ratio of R-2HG to S-2HG in primary human IDH2 mutant AML cells 24 hours after BAY1436032 treatment. Intracellular R-2HG/S-2HG ratios were calculated as percentage of DMSO (CTL) treatment (mean ± SEM, *n* = 3). (**C**) Representative FACS plots showing increased expression of myelomonocytic differentiation markers CD14 and CD15 on primary AML cells with different IDH1 mutations after *ex vivo* treatment with 1 □M BAY1436032 for 19 days. DMSO treatment was used as a control. Cells expressing CD14 and CD15 are marked by a gate and percentages of $CD14^+/CD15^+$ cells are given in the graph. (**c**) Quantification of IDH1 wild-type (wt) or IDH1 mutant primary AML cells expressing CD14 and CD15 after *ex vivo* treatment with DMSO or BAY1436032 (mean ± SEM). Treatment durations and numbers of patient samples examined are given in the graph. *, $P < 0.05$; **, $P < 0.01$.

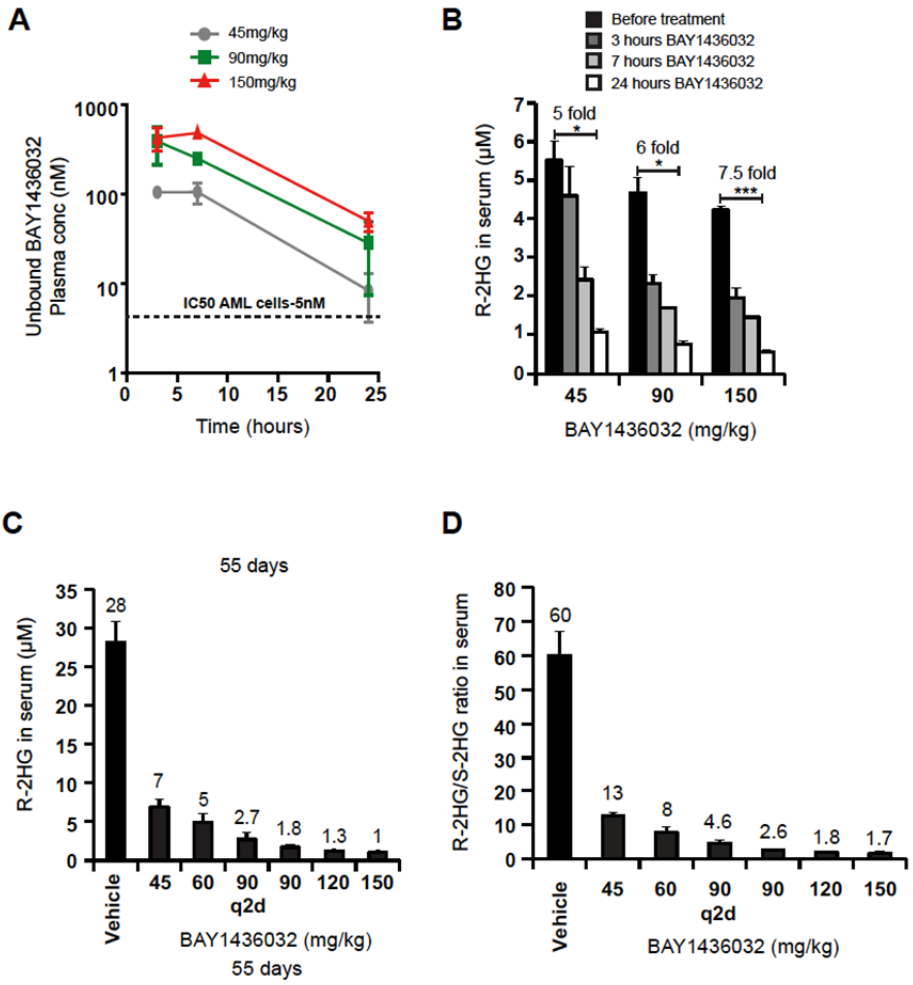

Supplementary Figure 2. BAY1436032 reduces R-2HG serum levels in an AML PDX mouse model *in vivo*. (**A**) BAY1436032 unbound plasma concentrations in PDX1-IDH1R132C mice treated with a single oral dose of 45, 90 or 150 mg/kg BAY1436032 (mean ± SEM of 2-3 animals/time point) at 3, 7 and 24 hours after treatment. The dashed line indicates the *in vitro* R-2HG/S-2HG ratio IC_{50} value in IDH1R132C mutant human primary AML cells. (**B**) R-2HG serum levels of PDX1-IDH1R132C mice treated with a single oral dose of 45, 90 or 150 mg/kg BAY1436032 at 3, 7 and 24 hours after treatment (mean ± SEM, n = 3). *, $P < 0.05$; ***, $P < 0.001$. (**C**) R-2HG serum levels of PDX1-IDH1R132C mice treated either daily with an oral dose of 45, 60, 90, 120 or 150 mg/kg or every alternate day with 90 mg/kg (90 q2) BAY1436032 at 55 days after treatment start (mean ± SEM, n = 6-10 animals per treatment group). (**D**) Ratio of R-2HG to S-2HG in serum of PDX1-IDH1R132C mice treated with BAY1436032. Animals were treated with daily oral doses of 45, 60, 90, 120 or 150 mg/kg or every alternate day with 90mg/kg BAY1436032 (indicated as 90 mg/kg, q2d in the graph). The R-2HG/S-2HG ratio was determined at 55 days after treatment start.

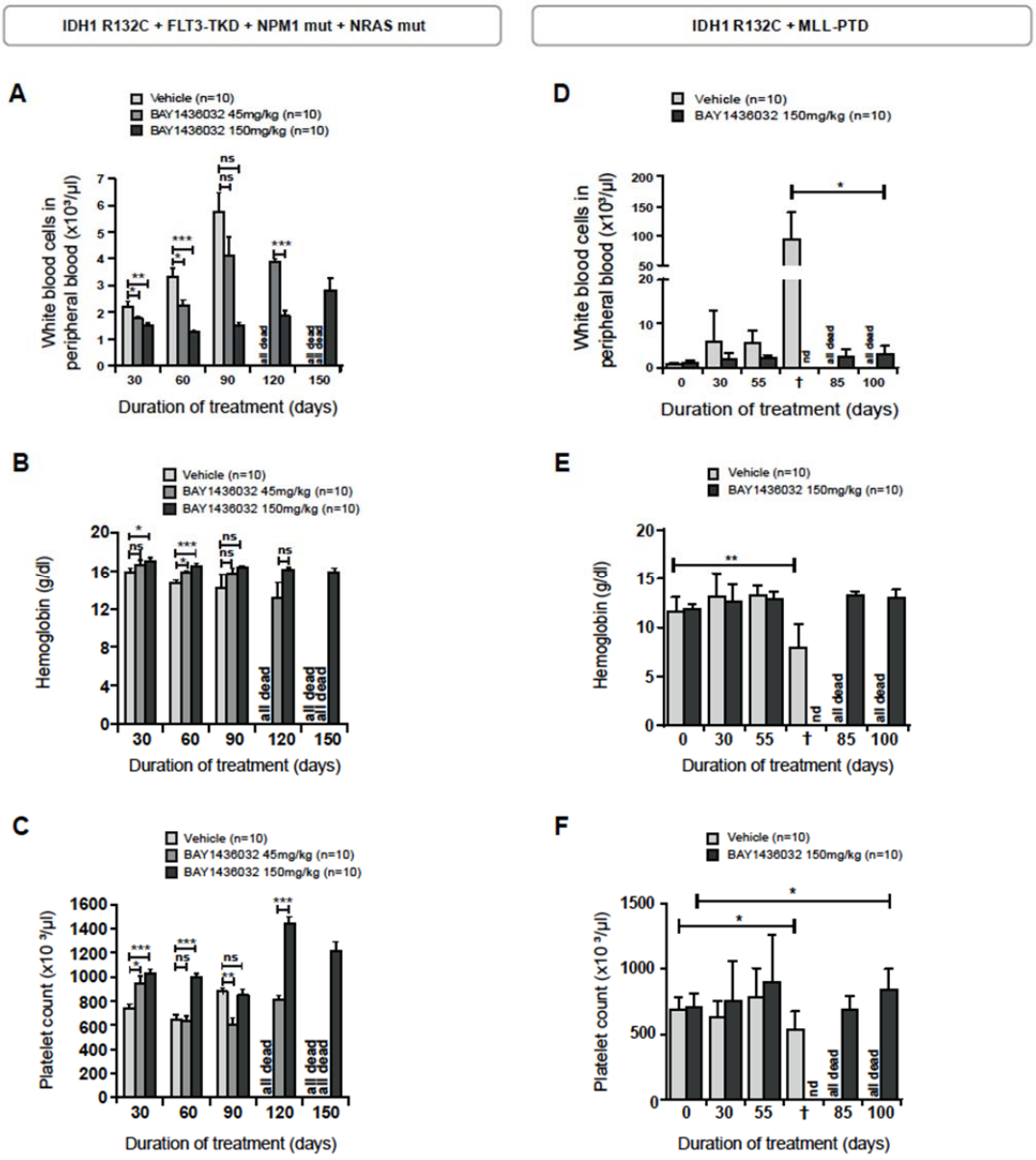

Supplementary Figure 3. Peripheral blood counts for the PDX1- and PDX2-IDH1R132C models. White blood cell counts (**A**), hemoglobin levels (**B**) and platelet counts (**C**) in peripheral blood at different time points during treatment with either 45 or 150 mg/kg BAY1436032 or vehicle of PDX1-IDH1R132C mice (mean ± SEM, *n* = 10). White blood cell counts (**D**), hemoglobin levels (**E**) and platelet counts (**F**) in peripheral blood at different time points during treatment with 150 mg/kg BAY1436032 or vehicle of PDX2-IDH1R132C mice (mean ± SD, *n* = 10). *, $P < 0.05$; **, $P < 0.01$; ***, $P < 0.001$; ns, not significant; nd, not determined; †, time of death.

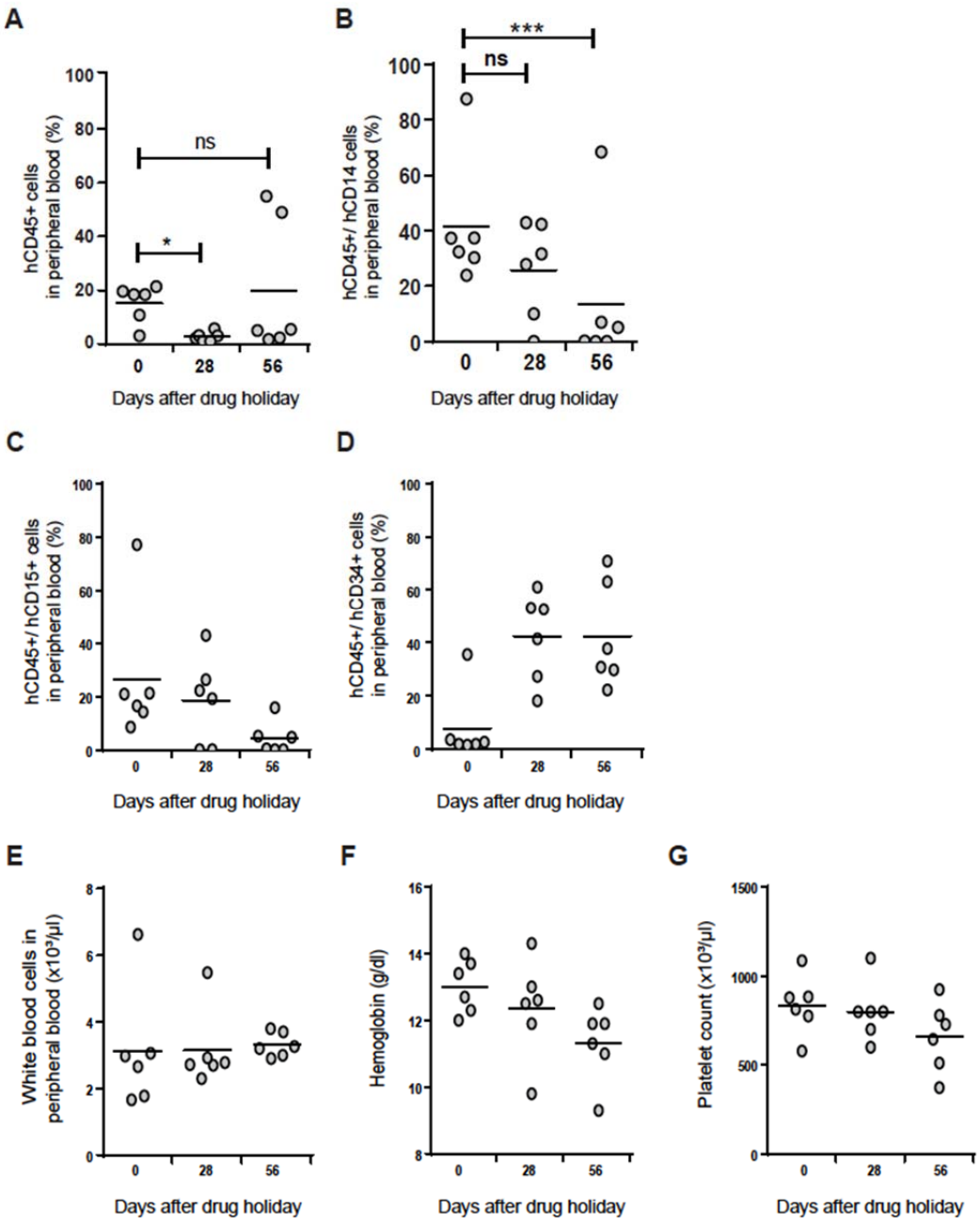

Supplementary Figure 4. Peripheral blood counts and immunophenotype for the PDX2-IDH1R132C model after treatment stop. Percentages of total hCD45$^+$ leukemic cells (**A**), hCD45$^+$/CD14$^+$ cells (**B**), hCD45$^+$/CD15$^+$ cells (**C**), hCD45$^+$/CD34$^+$ cells (**D**) as well as white blood cell counts (**E**), hemoglobin levels (**F**) and platelet counts (**G**) in peripheral blood of PDX2-IDH1R132C mice at day 100 after treatment start with 150 mg/kg BAY1436032 (0) and 28 and 56 days after termination of treatment (mean, n = 6). *, $P < 0.05$; ***, $P < 0.001$; ns, not significant.

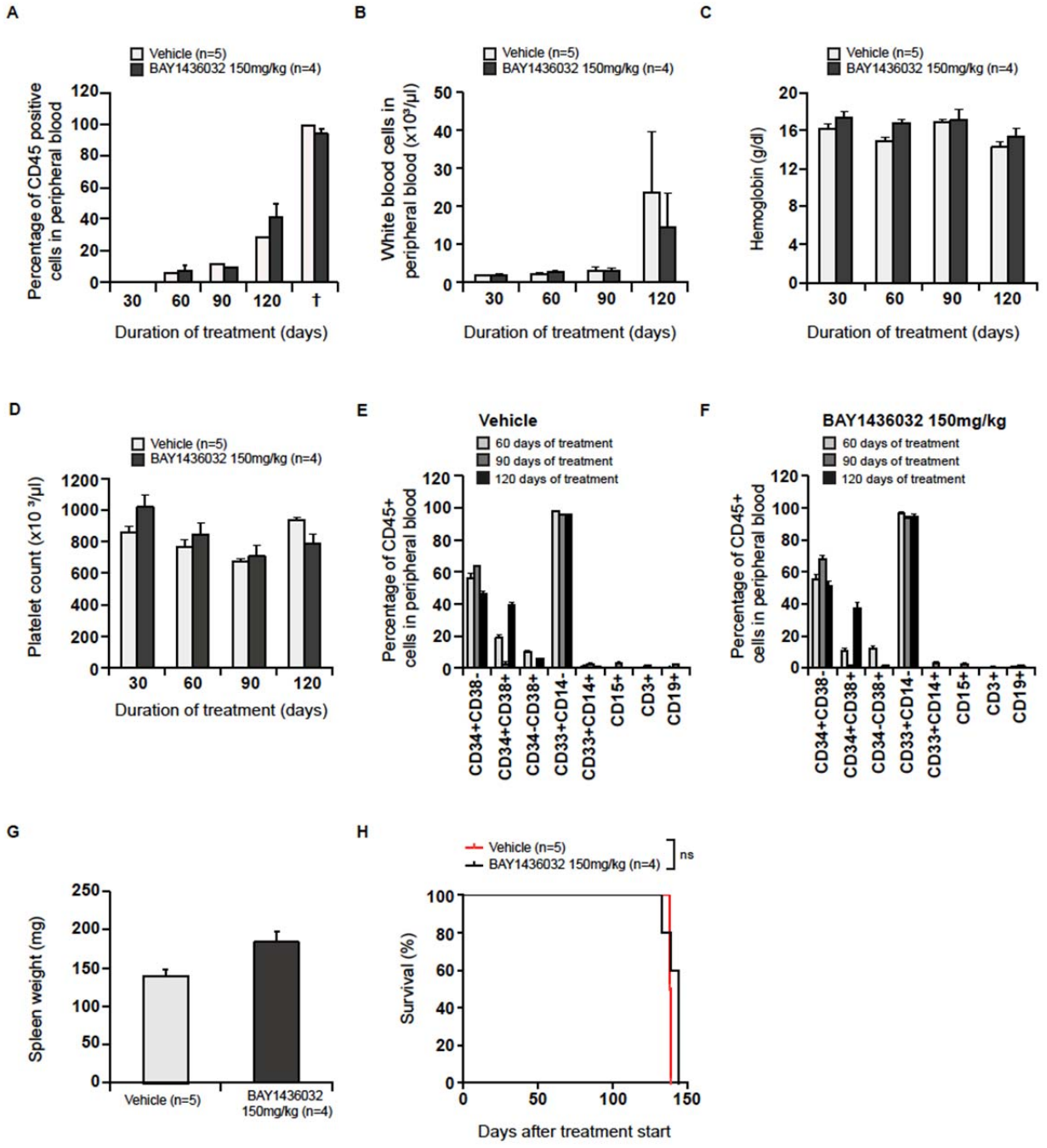

Supplementary Figure 5. BAY1436032 neither has anti-leukemic activity nor induces myeloid differentiation in an IDH1 wildtype AML PDX model *in vivo* (PDX3). (**A**) Engraftment of human wildtype IDH1 AML patient cells in peripheral blood of NSG mice at different time points after treatment with either vehicle or 150 mg/kg BAY1436032 (mean ± SEM, *n* = 4-5). (**B**) White blood cell counts in peripheral blood of PDX3 mice at different time points after treatment with either vehicle or 150 mg/kg BAY1436032 (mean ± SEM, *n* = 4-5). (**C**) Hemoglobin levels in peripheral

blood of PDX3 mice at different time points during treatment with either vehicle or 150 mg/kg BAY1436032 (mean ± SEM, *n* = 4-5). (**D**) Platelet counts in peripheral blood of PDX3 mice at different time points during treatment with either vehicle or 150 mg/kg BAY1436032 (mean ± SEM, *n* = 4-5). (**E**) Immunophenotype of $hCD45^+$ PDX3 cells in peripheral blood of mice after treatment with vehicle at the indicated time points (mean ± SEM, *n* = 5). (**F**) Immunophenotype of human PDX3 cells in peripheral blood of mice after treatment with 150 mg/kg BAY1436032 at the indicated time points (mean ± SEM, *n* = 4). (**G**) Spleen weight at the time of death of PDX3 mice treated with vehicle or 150 mg/kg BAY1436032 until death. (**H**) Survival of PDX3 mice treated with 150 mg/kg BAY1436032 or vehicle.

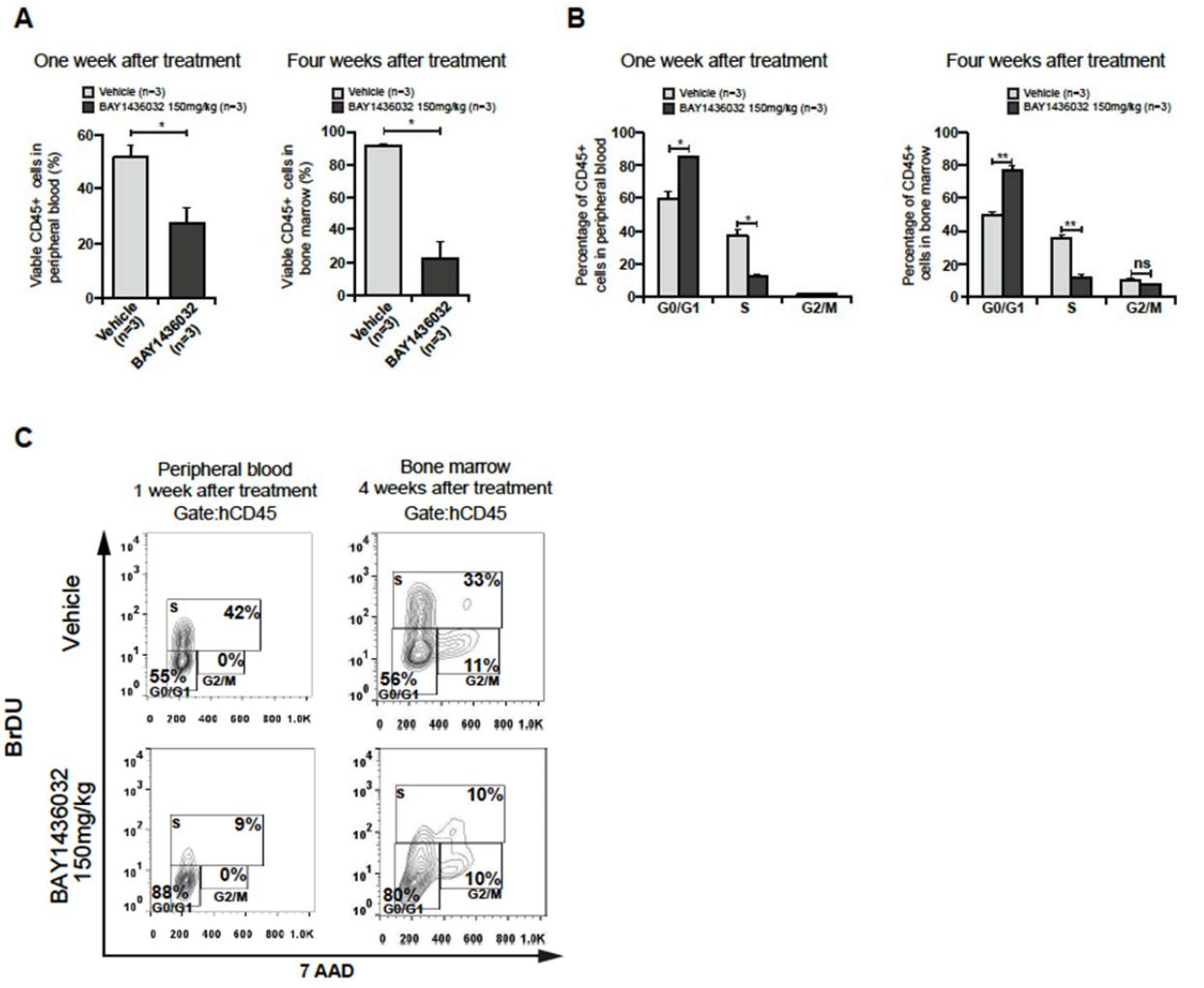

Supplementary Figure 6. Cell cycle distribution of PDX1-IDH1R132C AML cells treated with vehicle or BAY1436032 *in vivo*. Proportion of viable hCD45$^+$ cells (**A**) and their cell cycle distribution (**B**) in peripheral blood (left panels) and bone marrow (right panels) of PDX1-IDH1R132C mice treated with vehicle or 150 mg/kg BAY1436032 for 1 or 4 weeks, respectively (mean ± SEM, n = 3). (**C**) A representative FACS plot from peripheral blood (left panels) and bone marrow (right panels) of mice treated with either vehicle or 150 mg/kg BAY1436032. Results are shown as percentages of hCD45$^+$ cells. *, $P < 0.05$; **, $P < 0.01$; ns, not significant.

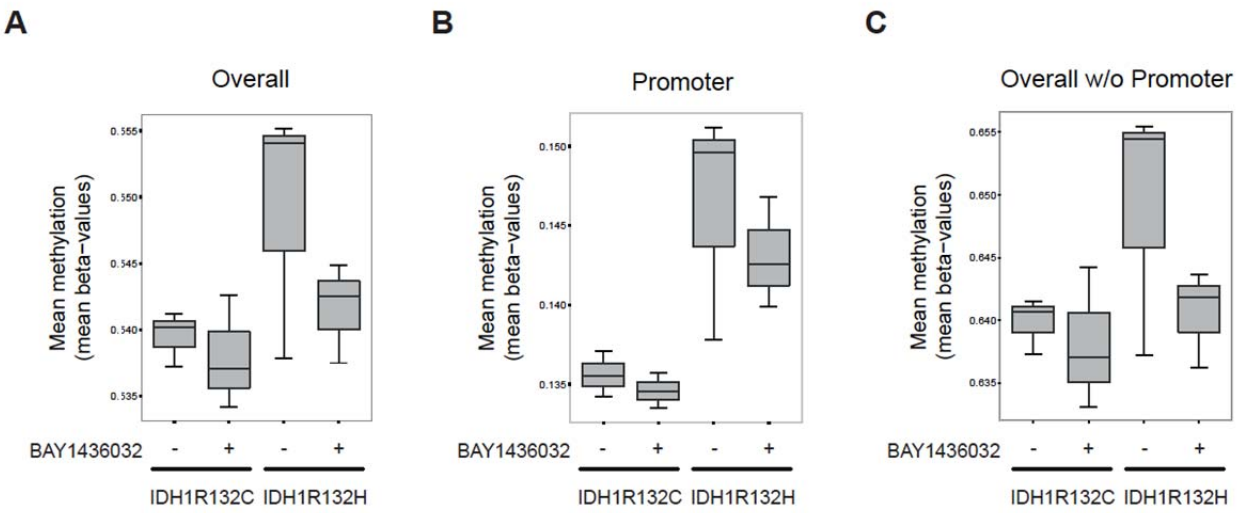

Supplementary Figure 7. DNA-methylation in primary IDH1R132C or IDH1R132H mutant AML cells treated with 500 nM BAY1436032 or DMSO for 14 days *ex vivo*. Boxes represent medians and quartiles with wiskers ranging from the highest to the lowest value. (**A**) Mean overall methylation rates. (**B**) Mean promoter methylation rates. (**C**) Mean methylation rates without promoter sites.

Table S1: Top 100 gene sets from gene ontology (C5).

Rank	GO term	NES	p Value	Classification
1	MYELOID_CELL_DIFFERENTIATION	1.694714	0	Differentiation
2	IMMUNE_RESPONSE	1.623525	0	Immune respose
3	IMMUNE_SYSTEM_PROCESS	1.604645	0	Immune respose
4	RESPONSE_TO_VIRUS	1.572526	0	Immune respose
5	RESPONSE_TO_OTHER_ORGANISM	1.565558	0	Others
6	CELLULAR_DEFENSE_RESPONSE	1.548541	0	Immune respose
7	ACTIN_FILAMENT_BINDING	1.548164	0	Cell morphogenesis/migration
8	GATED_CHANNEL_ACTIVITY	1.547899	0.19427402	Membrane ion transport
9	RESPONSE_TO_BIOTIC_STIMULUS	1.530246	0	Signalling/response to signal
10	LYMPHOCYTE_DIFFERENTIATION	1.515443	0	Differentiation
11	ANTIGEN_BINDING	1.514065	0	Cell membrane/receptor
12	VOLTAGE_GATED_CHANNEL_ACTIVITY	1.50669	0.19427402	Membrane ion transport
13	ION_CHANNEL_ACTIVITY	1.506279	0.19114688	Signalling/response to signal
14	DEFENSE_RESPONSE	1.503854	0	Immune respose
15	CELL_MATRIX_JUNCTION	1.502575	0.1017964	Cell morphogenesis/migration
16	IMMUNE_SYSTEM_DEVELOPMENT	1.501874	0	Others
17	HEMOPOIETIC_OR_LYMPHOID_ORGAN_DEVELOPMENT	1.495136	0	Others
18	METAL_ION_TRANSMEMBRANE_TRANSPORTER_ACTIVITY	1.494501	0.1888668	Membrane ion transport
19	VOLTAGE_GATED_CATION_CHANNEL_ACTIVITY	1.49399	0.19427402	Membrane ion transport
20	REGULATION_OF_MYELOID_CELL_DIFFERENTIATION	1.491281	0	Differentiation
21	METAL_ION_TRANSPORT	1.490976	0	Others
22	SUBSTRATE_SPECIFIC_CHANNEL_ACTIVITY	1.489688	0.19114688	Membrane ion transport
23	CATION_CHANNEL_ACTIVITY	1.486914	0.19348268	Membrane ion transport
24	NEGATIVE_REGULATION_OF_GROWTH	1.484249	0	Signalling/response to signal
25	LYMPHOCYTE_ACTIVATION	1.479304	0	Signalling/response to signal
26	HEMOPOIESIS	1.478447	0	Others
27	GROWTH_FACTOR_BINDING	1.47061	0	Cell membrane/receptor
28	INFLAMMATORY_RESPONSE	1.464875	0	Immune respose
29	RAS_GUANYL_NUCLEOTIDE_EXCHANGE_FACTOR_ACTIVITY	1.459358	0	Signalling/response to signal
30	CYSTEINE_TYPE_ENDOPEPTIDASE_ACTIVITY	1.456096	0	Others
31	PATTERN_BINDING	1.455917	0	Others
32	POTASSIUM_ION_TRANSPORT	1.452543	0	Membrane ion transport
33	PROTEINACEOUS_EXTRACELLULAR_MATRIX	1.449404	0.22920893	Cell morphogenesis/migration
34	EXTRACELLULAR_MATRIX_PART	1.449236	0.10386965	Cell morphogenesis/migration
35	MULTI_ORGANISM_PROCESS	1.440264	0	Others
36	ADHERENS_JUNCTION	1.433143	0.10261569	Cell morphogenesis/migration
37	LEADING_EDGE	1.432902	0	Others
38	OXIDOREDUCTASE_ACTIVITY_GO_0016705	1.427042	0	Metabolism
39	REGULATION_OF_IMMUNE_SYSTEM_PROCESS	1.424166	0	Signalling/response to signal
40	INTEGRIN_BINDING	1.423936	0	Signalling/response to signal
41	VOLTAGE_GATED_POTASSIUM_CHANNEL_ACTIVITY	1.420796	0.1888668	Membrane ion transport
42	RESPONSE_TO_WOUNDING	1.419603	0	Others
43	CYTOKINE_BINDING	1.416371	0	Cell membrane/receptor
44	MONOVALENT_INORGANIC_CATION_TRANSPORT	1.416094	0	Membrane ion transport
45	CATION_TRANSPORT	1.415467	0	Membrane ion transport
46	KINASE_BINDING	1.414887	0	Signalling/response to signal
47	INTERLEUKIN_RECEPTOR_ACTIVITY	1.408588	0	
48	POTASSIUM_CHANNEL_ACTIVITY	1.405675	0.10139165	Membrane ion transport
49	POSITIVE_REGULATION_OF_TRANSFERASE_ACTIVITY	1.404211	0.21984436	Signalling/response to signal
50	POSITIVE_REGULATION_OF_SIGNAL_TRANSDUCTION	1.398941	0	Signalling/response to signal
51	REGULATION_OF_RESPONSE_TO_STIMULUS	1.397106	0.0859375	Immune respose
52	POSITIVE_REGULATION_OF_RESPONSE_TO_STIMULUS	1.396956	0	Immune respose
53	PROTEASE_INHIBITOR_ACTIVITY	1.392857	0	Others
54	COLLAGEN	1.390439	0	others
55	VOLTAGE_GATED_POTASSIUM_CHANNEL_COMPLEX	1.389008	0.10261569	Membrane ion transport
56	CELLULAR_CATION_HOMEOSTASIS	1.387732	0	Membrane ion transport
57	ION_TRANSPORT	1.382729	0	Membrane ion transport
58	RESPONSE_TO_BACTERIUM	1.381623	0	Immune respose
59	REGULATION_OF_TRANSLATION	1.377123	0.08661418	Signalling/response to signal
60	EPIDERMIS_DEVELOPMENT	1.376866	0.1009901	Cell morphogenesis/migration
61	POSITIVE_REGULATION_OF_IMMUNE_RESPONSE	1.372746	0	Immune respose
62	B_CELL_ACTIVATION	1.372184	0	Immune respose
63	LOCOMOTORY_BEHAVIOR	1.371364	0	Cell morphogenesis/migration
64	ECTODERM_DEVELOPMENT	1.371204	0.10261569	Cell morphogenesis/migration
65	GENERATION_OF_NEURONS	1.370843	0.1009901	Cell morphogenesis/migration
66	IMMUNE_EFFECTOR_PROCESS	1.365987	0	Immune respose
67	RESPONSE_TO_EXTERNAL_STIMULUS	1.365088	0	Signalling/response to signal
68	DETECTION_OF_EXTERNAL_STIMULUS	1.364206	0.10472279	Signalling/response to signal
69	REGULATION_OF_CYTOKINE_BIOSYNTHETIC_PROCESS	1.363474	0	Signalling/response to signal
70	INTERLEUKIN_BINDING	1.362945	0	Immune respose
71	CYTOKINE_METABOLIC_PROCESS	1.36242	0	Metabolism
72	REGULATION_OF_SIGNAL_TRANSDUCTION	1.361664	0	Signalling/response to signal
73	SUGAR_BINDING	1.361331	0.1009901	Others

74	EPIDERMAL_GROWTH_FACTOR_RECEPTOR_SIGNALING_PATHWAY	1.353155	0	Signalling/response to signal
75	HEPARIN_BINDING	1.351716	0.1050505	Others
76	LEUKOCYTE_DIFFERENTIATION	1.34906	0	Differentiation
77	EXTRACELLULAR_MATRIX	1.347929	0.3184584	Cell morphogenesis/migration
78	LEUKOCYTE_ACTIVATION	1.344039	0	Immune respose
79	HEMATOPOIETIN_INTERFERON_CLASSD200_DOMAIN_CYTOKINE_RECEPTOR_ACTIVITY	1.342045	0	Signalling/response to signal
80	CELL_ACTIVATION	1.341972	0	Signalling/response to signal
81	VITAMIN_METABOLIC_PROCESS	1.338895	0.1049505	Metabolism
82	PHAGOCYTOSIS	1.338792	0	Immune respose
83	ENZYME_INHIBITOR_ACTIVITY	1.337544	0	Others
84	CATION_HOMEOSTASIS	1.337213	0	Membrane ion transport
85	NEURON_DIFFERENTIATION	1.336129	0.10139165	Differentiation
86	CELL_SURFACE	1.334607	0	Cell morphogenesis/migration
87	CATION_TRANSMEMBRANE_TRANSPORTER_ACTIVITY	1.334079	0.22376238	Signalling/response to signal
88	G_PROTEIN_SIGNALING_COUPLED_TO_CYCLIC_NUCLEOTIDE_SECOND_MESSENGER	1.33406	0.22736418	Signalling/response to signal
89	REGULATION_OF_IMMUNE_RESPONSE	1.333079	0	Immune respose
90	RUFFLE	1.330985	0	Others
91	ENZYME_ACTIVATOR_ACTIVITY	1.3305	0	Others
92	DI___TRI_VALENT_INORGANIC_CATION_TRANSPORT	1.32663	0	Membrane ion transport
93	POSITIVE_REGULATION_OF_I_KAPPAB_KINASE_NF_KAPPAB_CASCADE	1.325284	0.08249497	Signalling/response to signal
94	REGULATION_OF_ANGIOGENESIS	1.32428	0	Signalling/response to signal
95	REGULATION_OF_I_KAPPAB_KINASE_NF_KAPPAB_CASCADE	1.32414	0.08453608	Signalling/response to signal
96	G_PROTEIN_SIGNALING_COUPLED_TO_CAMP_NUCLEOTIDE_SECOND_MESSENGER	1.320581	0.1030303	Signalling/response to signal
97	SYNAPTIC_TRANSMISSION	1.319344	0.22465208	others
98	ION_TRANSMEMBRANE_TRANSPORTER_ACTIVITY	1.318397	0.22376238	Signalling/response to signal
99	I_KAPPAB_KINASE_NF_KAPPAB_CASCADE	1.317905	0.08453608	Signalling/response to signal
100	NEUROLOGICAL_SYSTEM_PROCESS	1.31494	0.31589538	Others

Cell membrane/receptor	4
Cell morphogenesis/migration	11
Differentiation	5
Immune response	16
Membrane ion transport	16
Metabolism	3
Signalling/response to signal	26
Others	19

Table S2: Top 100 gene sets from transcription factor collection (C3).

Enriched in BAY1436032 treated cells			
Rank	GO term	NES	p Value
1	NFKB_Q6_01	1.549157	0.08130081
2	NFKAPPAB65_01	1.467269	0
3	ELF1_Q6	1.453206	0.108050846
4	CREL_01	1.435299	0.07984032
5	NFKB_Q6	1.374188	0
6	EVI1_03	1.340694	0.1364562
7	AML_Q6	1.308359	0.08146639
8	AP4_01	1.29971	0
9	NFKB_Q6_01	1.293088	0.08146639
10	AP1_Q6	1.289417	0
11	AP1_Q6_01	1.286441	0
12	AP1_01	1.283384	0
13	NFKAPPAB_01	1.282354	0.08368201
14	RORA2_01	1.276807	0
15	OCT1_B	1.276412	0.13508065
16	NFAT_Q4_01	1.274926	0
17	PU1_Q6	1.269298	0.10559006
18	AP1_Q4_01	1.256024	0
19	AP1FJ_Q2	1.249369	0
20	LXR_Q3	1.240383	0
21	OCT_Q6	1.23526	0.09146342
22	AP1_Q2	1.227718	0
23	NRSF_01	1.22642	0.30938125
24	AP2REP_01	1.224327	0.1814433
25	AP2ALPHA_01	1.223263	0
26	PAX2_02	1.221806	0.099609375
27	PPARA_01	1.218054	0.18503937
28	OLF1_01	1.211493	0
29	NFE2_01	1.205931	0.08213552
30	NFKB_C	1.19119	0.18495935
31	HNF4_01	1.184694	0.07984032
32	ETS2_B	1.176701	0.18685831
33	TCF11MAFG_01	1.174994	0.105906315
34	OCT1_01	1.171519	0.32157677
35	FOXJ2_01	1.16834	0.17276423
36	AP1_Q4	1.166869	0.08213552
37	STAT5B_01	1.166118	0.08080808
38	EVI1_05	1.163897	0.22626263
39	AP1_C	1.162422	0.08829569
40	HNF3B_01	1.161083	0.40456432
41	IK2_01	1.160338	0.08146639
42	NERF_Q2	1.159455	0.19037656
43	AML_Q6	1.156484	0.17311609
44	LFA1_Q6	1.155453	0.103869654
45	LBP1_Q6	1.148906	0.13562752
46	MYOGENIN_Q6	1.145445	0.31376517
47	HNF4_Q6	1.13998	0.08213552
48	AP1_Q2_01	1.139347	0.31504065
49	ATF3_Q6	1.1366	0.16330644
50	TBP_01	1.134128	0.08368201
51	OCT1_Q5_01	1.133251	0.30876493
52	E2A_Q2	1.132997	0.3131313
53	AP4_Q6	1.130244	0.3051181
54	HSF2_01	1.1293	0.17515275

Depleted in BAY1436032 treated cells			
Rank	GO term	NES	p Value
1	E2F_Q6	-1.50848	0
2	E2F_Q3_01	-1.49115	0
3	E2F_Q4	-1.48481	0
4	E2F1_Q3	-1.48473	0
5	E2F1_Q4_01	-1.48101	0
6	E2F1DP1RB_01	-1.45728	0
7	E2F1_Q6	-1.45677	0
8	E2F4DP1_01	-1.4561	0
9	E2F_Q3	-1.45502	0
10	E2F1DP1_01	-1.44613	0
11	E2F1DP2_01	-1.44613	0
12	E2F4DP2_01	-1.44613	0
13	E2F_02	-1.44491	0
14	E2F1DP2_01	-1.44483	0
15	E2F_Q6_01	-1.41932	0
16	E2F_Q4_01	-1.41899	0
17	E2F1_Q6_01	-1.38848	0.091816
18	E2F1_Q4	-1.36816	0
19	E2F_03	-1.36653	0
20	MYCMAX_B	-1.31681	0
21	E2F_01	-1.30165	0.185106
22	E2F1_Q3_01	-1.19712	0.120553
23	PAX6_01	-1.18269	0.185111
24	PPARG_01	-1.17977	0.114458
25	NFMUE1_Q6	-1.15347	0
26	HIF1_Q3	-1.14634	0.304255
27	ELK1_02	-1.12044	0.417795
28	ARNT_01	-1.11311	0.316406
29	IRF2_01	-1.10338	0.179167
30	NMYC_01	-1.09169	0.211934
31	MYCMAX_01	-1.07337	0.296296
32	IRF_Q6	-1.0398	0.397059
33	YY1_Q6	-1.02855	0.394059
34	CREB_Q3	-1.01851	0.51068
35	YY1_Q6	-0.99951	0.409543
36	SOX5_01	-0.98128	0.511156
37	MAX_01	-0.97865	0.597194
38	AHR_Q5	-0.96772	0.613924
39	WHN_B	-0.94526	0.636008
40	NFY_Q6_01	-0.93022	0.599214
41	TAL1ALPHAE47_01	-0.9194	0.585987
42	NRF1_Q6	-0.91932	0.683468
43	CREB_02	-0.91573	0.596869
44	USF_C	-0.90148	0.530612
45	ISRE_01	-0.90123	0.686117
46	IRF1_01	-0.88473	0.710372
47	E47_02	-0.88198	0.680162
48	CREB_Q2	-0.88177	0.630137
49	CREB_Q2_01	-0.87799	0.515091
50	USF_Q6	-0.87692	0.688588
51	SOX9_B1	-0.87402	0.895966
52	NFY_01	-0.86445	0.801587
53	E2F_Q2	-0.86324	0.769384
54	CREB_Q4	-0.85341	0.616858

55	COREBINDINGFACTOR_Q	1.124872	0.17219917
56	SREBP1_02	1.123526	0.21414538
57	ER_Q6_02	1.12089	0.1364562
58	FOXJ2_02	1.1206	0.087649405
59	HSF_Q6	1.116692	0.26035503
60	EVI1_02	1.11416	0.3029703
61	POU3F2_01	1.111484	0.31
62	EVI1_06	1.110257	0.29568788
63	POU1F1_Q6	1.110015	0.18016194
64	HNF1_01	1.109511	0.31504065
65	PPARA_02	1.109026	0.20977597
66	STAT_Q6	1.107642	0.17408907
67	CEBP_Q3	1.107484	0.31380752
68	PU1_Q6	1.106111	0.26242545
69	PAX4_03	1.105298	0.22357723
70	FREAC7_01	1.103534	0.16831683
71	CEBP_Q2_01	1.101911	0.17741935
72	PEA3_Q6	1.101784	0.1809145
73	NKX25_02	1.101136	0.30876493
74	CHOP_01	1.098637	0.18699187
75	AML1_Q6	1.09783	0.2611336
76	AML1_01	1.09783	0.2611336
77	POU6F1_01	1.097194	0.31504065
78	STAT5A_03	1.09543	0.17364016
79	AP2GAMMA_01	1.093027	0.103658535
80	CP2_02	1.092607	0.2219917
81	TEF1_Q6	1.090142	0.30451867
82	FXR_Q3	1.089518	0.43983403
83	HSF1_01	1.088615	0.19037656
84	EGR2_01	1.087752	0.22417153
85	ICSBP_Q6	1.087551	0.08921162
86	TCF11MAFG_01	1.083036	0.27104723
87	NFE2_01	1.082366	0.27104723
88	BACH1_01	1.081027	0.3131313
89	CACCCBINDINGFACTOR_C	1.079577	0.31504065
90	RSRFC4_01	1.076364	0.26556018
91	STAT_01	1.073433	0.17991632
92	OCT_C	1.072863	0.40243903
93	PXR_Q2	1.071969	0.30214426
94	AP4_Q5	1.071427	0.40936863
95	HNF1_C	1.0713	0.31504065
96	GATA_Q6	1.068251	0.3081511
97	FXR_IR1_Q6	1.067714	0.36252546
98	HNF6_Q6	1.067684	0.33789062
99	LHX3_01	1.067227	0.3131313
100	FAC1_01	1.066688	0.33789062

55	CETS1P54_01	-0.84726	0.594118
56	EGR3_01	-0.84047	0.6875
57	MYC_Q2	-0.82839	0.716327
58	YY1_02	-0.8277	0.673956
59	TAL1BETAE47_01	-0.8263	0.72327
60	GABP_B	-0.82577	0.811133
61	AP2_Q6_01	-0.82574	0.698189
62	GATA1_01	-0.82374	0.720322
63	SP1_Q6	-0.82175	0.703557
64	NRF2_01	-0.81233	0.697813
65	HIF1_Q5	-0.81108	0.902778
66	MYCMAX_03	-0.80762	0.685547
67	MYB_Q5_01	-0.80638	0.90411
68	MYCMAX_02	-0.79647	0.710204
69	PPAR_DR1_Q2	-0.79173	0.902778
70	ARNT_02	-0.78492	0.773879
71	CEBPGAMMA_Q6	-0.78129	0.822938
72	MEF2_04	-0.77963	0.562753
73	MIF1_01	-0.77813	0.9
74	CMYB_01	-0.77789	0.617706
75	USF_01	-0.77785	0.679921
76	NFY_C	-0.77623	0.707819
77	E4BP4_01	-0.76944	0.901408
78	GRE_C	-0.76601	0.899384
79	ATF4_Q2	-0.76572	0.806262
80	RFX1_02	-0.7544	0.706122
81	ZF5_B	-0.74274	0.900609
82	SRY_02	-0.74239	0.897275
83	CREB_01	-0.73745	0.680077
84	HOX13_01	-0.73594	0.686508
85	E4F1_Q6	-0.72884	0.625243
86	TEF_Q6	-0.71747	0.90411
87	CREBP1CJUN_01	-0.71633	0.802395
88	PAX2_01	-0.7151	0.809917
89	ATF_01	-0.71046	0.904669
90	AR_03	-0.70031	0.795031
91	STAT1_02	-0.68744	0.90121
92	GR_01	-0.68696	0.903353
93	PAX3_B	-0.68005	0.906844
94	NKX3A_01	-0.67214	0.800821
95	NKX22_01	-0.67156	0.901408
96	STAT1_01	-0.66518	0.716327
97	HMX1_01	-0.65882	0.783673
98	CDPCR1_01	-0.65413	0.90081
99	TGIF_01	-0.65198	0.901408
100	SREBP1_01	-0.63183	0.904483